1-1-2010

Terrestrial and Marine Geobiophysical Spatial Analysis and Modeling of Phytoplankton and Nutrients in Haifa Bay, Israel

Sinaya Dayan
Sinaya77@yahoo.com

Terrestrial and Marine Geobiophysical Spatial Analysis and Modeling of Phytoplankton and Nutrients in Haifa Bay, Israel.

Thesis Submitted to
The Graduate College of
Marshall University

In partial fulfillment of
The requirements for the degree of
Master of Science in Physical Science
With an emphasis in Geobiophysical Modeling

By

Sinaya Dayan

Committee Members:
Professor James O. Brumfield, Ph.D., Thesis Advisor
Professor Ralph E. Oberly, Ph.D., Graduate Program Coordinator
Professor Nicola Orsini, Ph. D., Physics Department Chair

Marshall University

August 2010

Abstract

Haifa Bay, Israel, is considered one of the most polluted environments in the nation. The bay water is enriched with nutrients and shows elevated levels of phytoplankton biomass. This requires continuous data collection to monitor productivity. The objectives of these remote sensing geobiophysical models were to (1) create a terrestrial model component to identify sources for the elevated levels of nutrients in the bay, and (2) marine model component to validate remote sensing algorithms for the detection of Chlorophyll in an oceanic setting. Methods included Spatial Analysis, Principal Component Analysis, Unsupervised Classification, Map Algebra, Band Ratios, and Statistical Regression of reflection values against chlorophyll *In Situ* concentration measurements. The examination of the relationship between *in situ* measured chlorophyll concentrations and reflectance values included several models: linear, polynomial, exponential, and power transformations Results of the terrestrial model component validated the assumption that diffuse introduction of nutrient is mainly attributed to urban, industrial, and agricultural regions and intensive anthropogenic activity around the bay. The aquatic model component tested ocean color algorithms using ETM+ and MERIS data, which achieved results. ETM+ algorithm (TM2-TM3)/TM1 resulted in high correlation coefficient (R^2=0.8255) and was found suitable for the detection of low chlorophyll concentration <3mg/m^3. MERIS reflectance ratio R510/R560 was found most accurate and achieved high correlation between measured and reflected values (R^2=0.8428). The terrestrial and the marine components of the geobiophysical models provide an alternative, effective approach to the common monitoring techniques.

Keywords: Haifa Bay, Runoff Coefficient, Unsupervised Classification, Spatial Analysis, Ocean Color, Chlorophyll, Remote sensing, Nutrient Enrichment, Eutrophication, MERIS, ETM+.

Acknowledgements

The author would like to thank many people for their support, guidance, and encouragement. Dr. James Brumfield and Dr. Ralph Oberly, for a unique program, and the unlimited possibilities it presents. Thanks for a world of opportunities. To Dr. Nicola Orsini, thanks for taking an important part in the process. To Mike Orr, who had the patience to teach, the knowledge to share, and a contagious passion for the field. Many thanks for all the help. To Chandra Inglis-Smith, for the support, care, and direction. To Juan de Dios Barrios, thanks for many brain storming sessions. To Dr. Pamela Hamilton for the hours spent reading the study material, and for her genuine desire to enhance and contribute to the research. To LeAndria Reed, thanks for constant reminders and positive presence. To Linda Delaney, for reducing the financial stress factor, and keeping the researcher focused on what's important. Thanks so much! To Rahall Transportation Institute, thank you for being a challenging workplace and for providing an ideal research platform. To Dr. Richard Bagley, thanks for the great opportunity and for a wonderful professional journey at RTI. To the researcher's family, thanks for much needed support and encouragement during this long process. To Trace, for everything that you are, Thanks!

Table of Contents

List of Figures

List of Tables

List of Equations

CHAPTER I

Introduction

Overview

The Israeli Mediterranean coast, particularly around Haifa Bay, is characterized by intensive industrial activity and increasing population pressure around the coastal zone. Such dominating forces coupled with the negligence to alleviate the effects of such activity contributed to increasing influx of pollutants and nutrient enrichment into the coastal waters. The excessive anthropogenic activity led to extreme environmental impact: destruction and alteration of habitats, deterioration and contamination of ground water, coastal eutrophication, and the development of Harmful Algal Bloom (NMEMP, 2004).

The Israeli National effort in monitoring the water quality and productivity in the marine biosphere, regulating practices of wastewater discharge, and mitigating the environmental impact, requires extensive collection of *In Situ* measurements, which is a time consuming and a costly option. Remote sensing provides a collection platform with field sampling by which water quality and ocean health are assessed. The technology not only makes it possible to observe events in remote and difficult to access areas, but is also a practical solution to the common monitoring alternatives, as it simultaneously enables frequent sampling and provides a source for synoptic data at low cost (Gitelson et al., 1996). Ocean color in particular is a method of assessing the health of the oceanic environment by measuring biological activity through its optical characteristics. Phytoplankton or more precisely the active pigment contained in the cell, the chlorophyll, is considered a good indicator of ocean health and overall productivity (CCRS,

2008). The ability to map spatial and temporal patterns of ocean color provides important insights into fundamental processes and properties of the marine biosphere.

Marine Geospatial Biosphere Research Area: Haifa Bay

The research focused on Haifa Bay as seen in figure 1. Haifa is the third-largest metropolitan area in Israel, and the largest in Northern Israel. The Israeli Central Bureau of Statistics reported a population of almost 300,000, and a population density measured at 4,164 residents per km^2 (CBS, 2007). The Bay covers an area of 63.7 km^2 and boasts the largest of three major seaports on the Israeli Mediterranean coastline. It is known for the heavy industrial activity such as the oil refineries, petrochemical, chemical and biochemical plants (Figure 1) (Patience, 2006). The diverse industry, widespread marine and terrestrial agriculture, and a hydrologic system that effectively transports inputs from surface runoff, affect the quality of the coastal waters by the introduction of heavy loads of anthropogenic contaminators and nutrients (Gitelson et al., 1996).

Hydrology and topography are two dominating forces in the introduction of contaminators and nutrients into the Bay. The regional topography (Figure 2) dictates basin patterns, dividing drainage to the Jordan River in the east, and the Dead Sea from drainage to the Mediterranean in the west. The drainage basins of the major rivers and tributaries are vast, flow over heterogeneous land cover and land use, and introduce significant quantities of anthropogenic materials into Israel's Mediterranean coastal waters. The 70 km long Kishon River drains an area of 1110 km^2, which is the second largest catchment area of all coastal rivers (Kishon River Authority, 2007). The basin covers parts of the Palestinian territory, and travels through the Jezreel Valley, the agricultural heartland of the country, through a narrow rift, that is commonly

known as the Kishon rift, and then empties into the Mediterranean at Haifa Bay, as in Figure 2(IMEP, 2005).

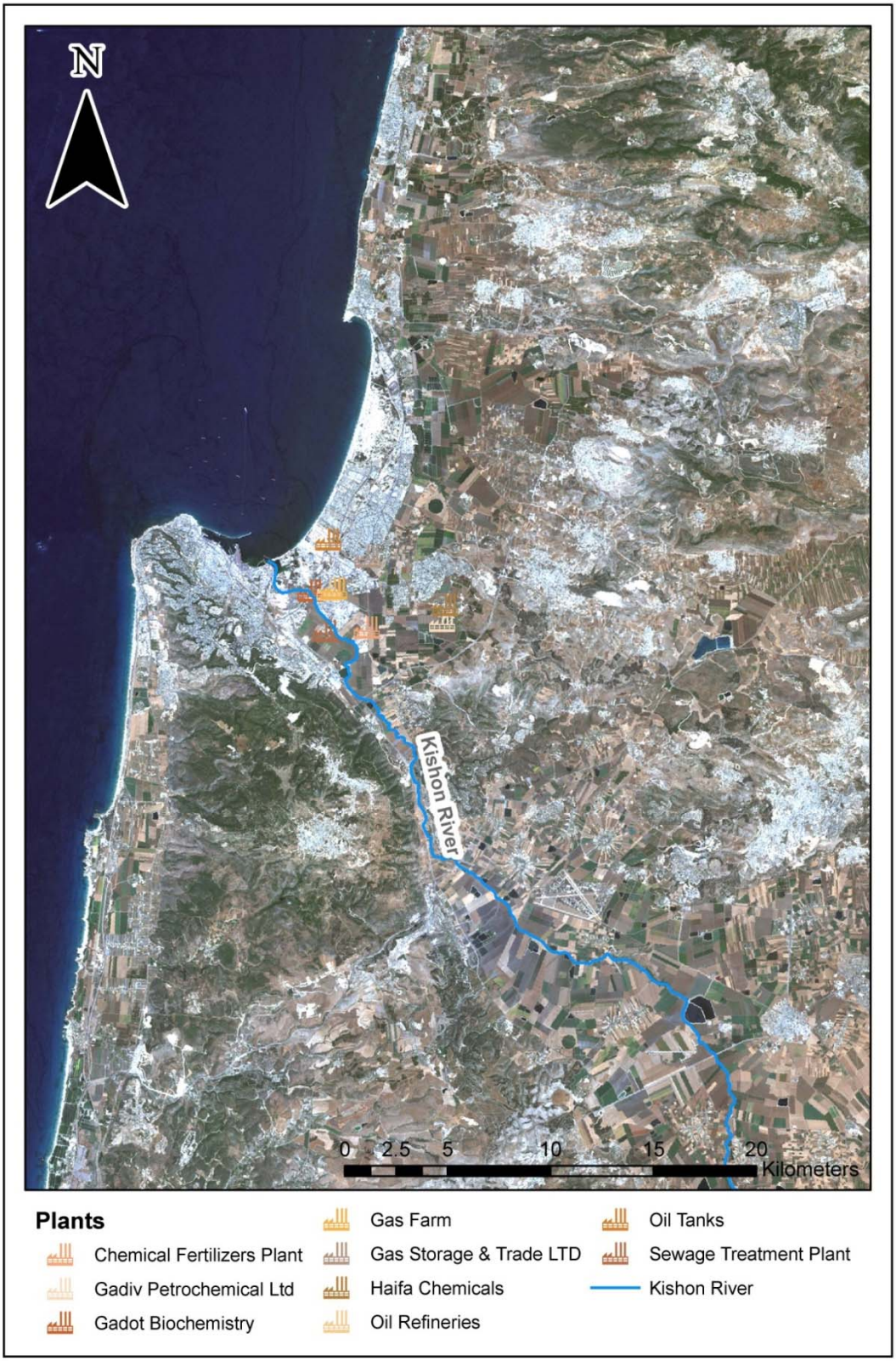

Figure 1: Haifa Bay Industrial Zone, ETM+ May 21 2000

Source: Sinaya Dayan, 08/01/09

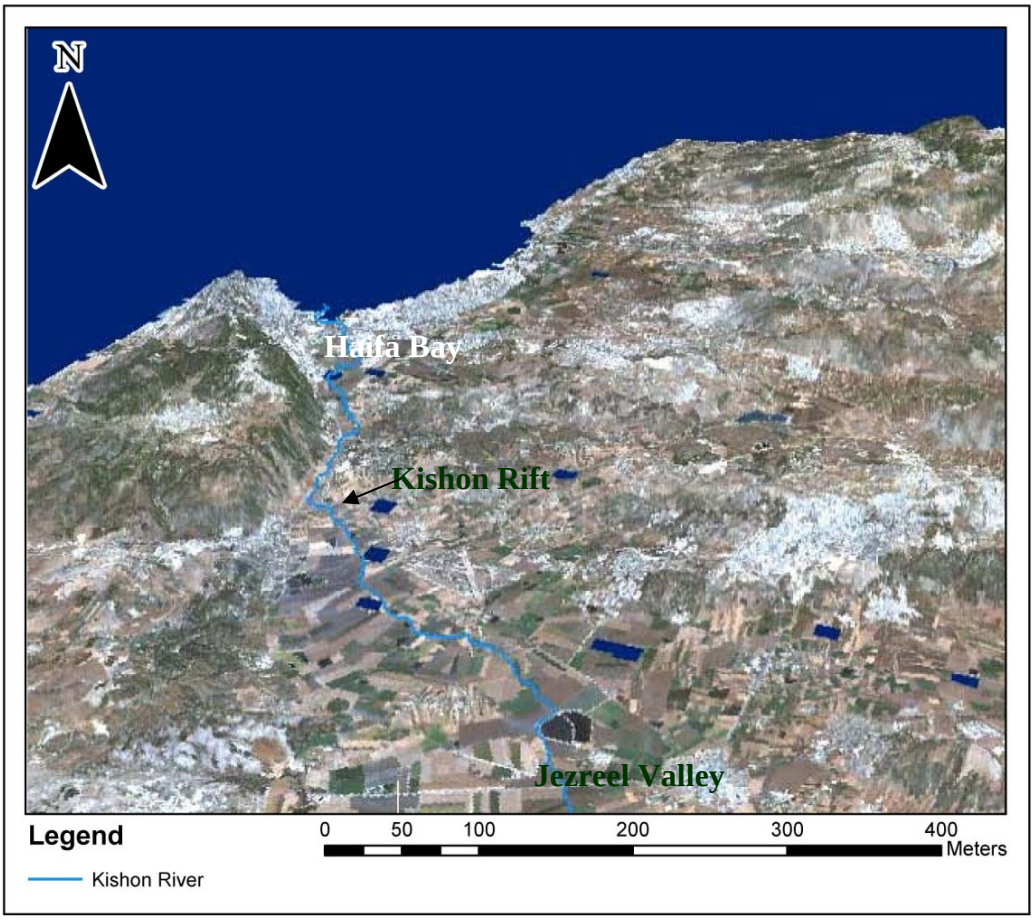

Figure 2: 3D Terrain Model of the Bay Region, ETM+ May 21 2000

Source: Sinaya Dayan, 08/01/09

The upper reaches of the Kishon contains mainly reclaimed water and agricultural runoff, while the lower reaches have been subjected to heavy pollution, originated in both municipal wastewaters and industrial effluents, discharged into the river. Additionally, as the lower part of the river flows through the heart of the metropolitan area, it drains urban runoffs while adding to the extreme pressure on the ecological system (Kishon River Authority, 2007). Consequently, the Kishon River was considered the most polluted river in Israel, as it shows increase in nutrients levels, especially Nitrates, (Figures 3, 4) which in turn amplifies the primary production of the system (IMEP, 2005; Herut & Kress, 1997). Although environmental regulations greatly

contributed to the decreasing trend of nutrient discharge into the river over the years, the inspected high levels of dissolved inorganic nutrients such as nitrogen and phosphorous still represent a high degree of pollution by international environmental criteria (NMEMP, 2004).

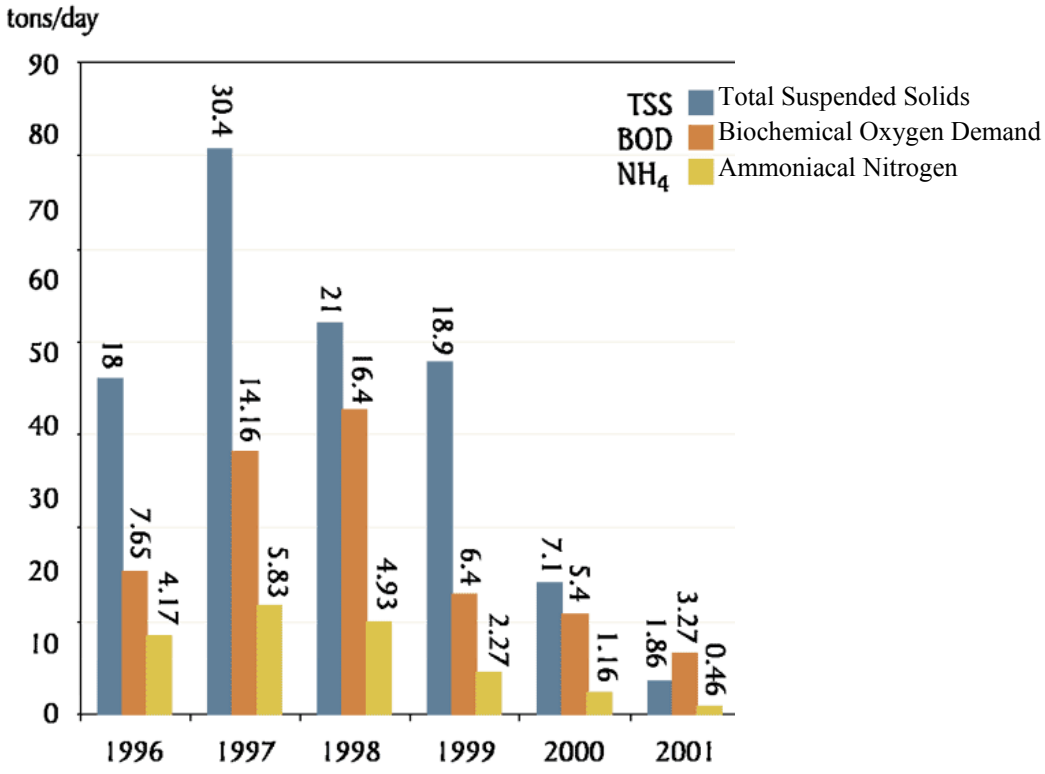

Figure 3: Discharge of BOD, TSS and NH4 to the Kishon River
Source: Kishon River Authority, 2007

Remote sensing technology offers a variety of sensor systems for acquiring information on the Open Ocean and coastal region. The collected data are used in global or regional modeling and monitoring, and allow both quantitative as well as qualitative representations of environmental phenomena.

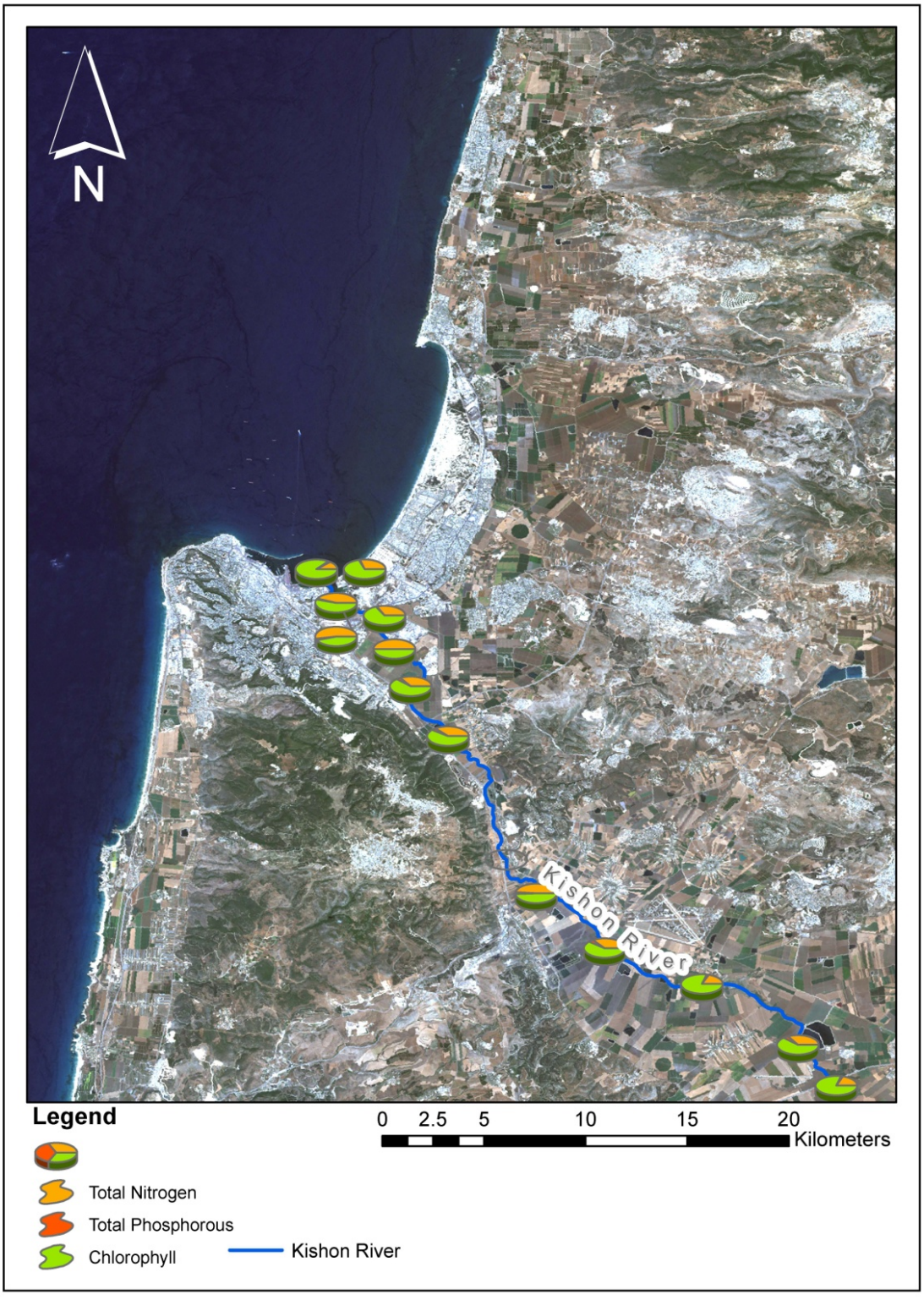

Figure 4: Total Nitrogen, Phosphorous, and Chlorophyll in the Kishon River, ETM+ May 21 2000

Source: Sinaya Dayan, 08/01/09

The Eastern Mediterranean: Geospatial Regional Analysis

The Mediterranean is an almost completely enclosed basin situated at the northern boundary of the desert climatic belt. It is connected to the Atlantic Ocean by the narrow and shallow Strait of Gibraltar with a maximum depth of 270 meters (Figures 5, 6). The continuous inflow of surface water from the Atlantic Ocean, through the Strait of Gibraltar, is the sea's major source of replenishment and water renewal (Kenneth et al., 2003).

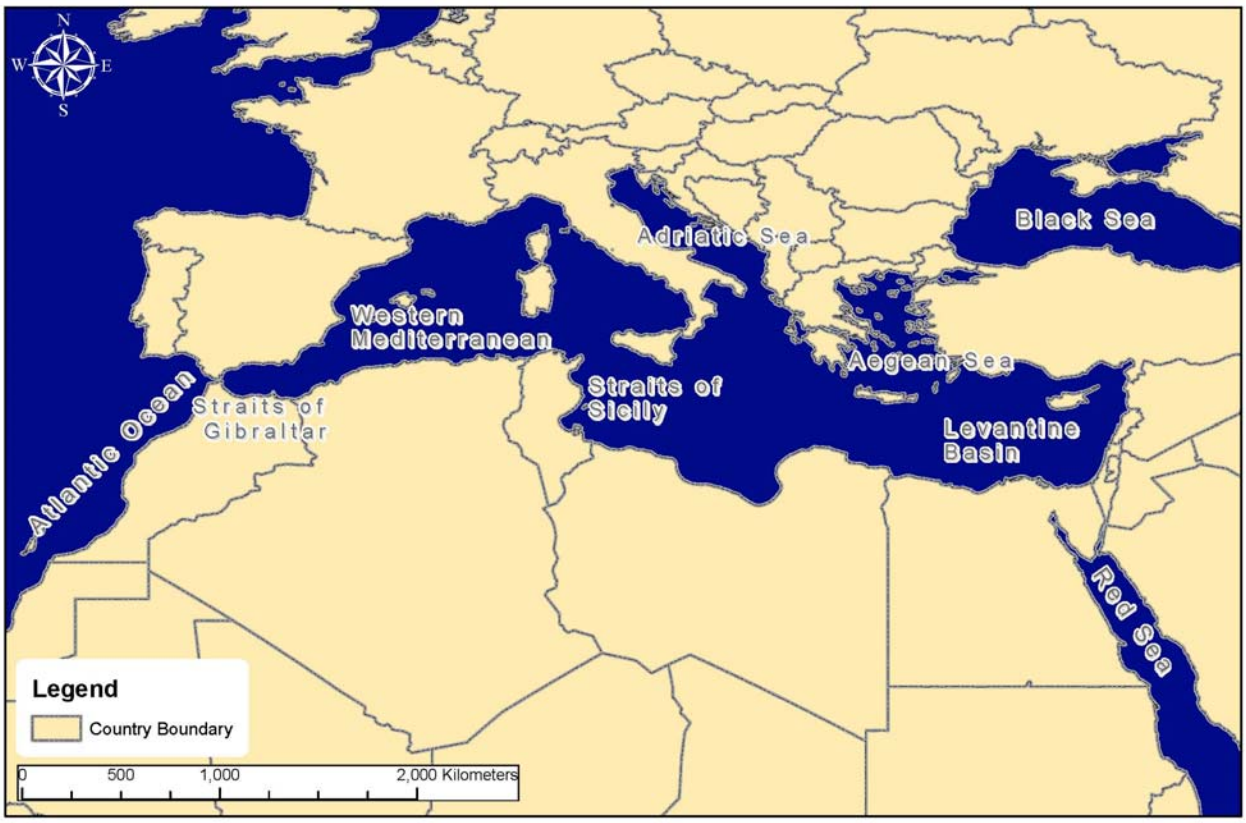

Figure 5: Mediterranean Basin

Source: Sinaya Dayan, 08/01/09

The Mediterranean, in general, and the Eastern Mediterranean, in particular, is characterized by high evaporation and loss of water, which is compensated by the net inflow of the Atlantic waters. The thermohaline circulation in the region is described as a two-layer

system; eastward inflow of lower salinity and lighter surface water from the Atlantic Ocean is replaced by deeper westward outflow of higher salinity, denser, intermediate waters as in Figure 6 (Malanotte-Rizzoli, 2008; Huertas et al., 2009). The exchange of water with the Atlantic effectively transports nutrients from the Mediterranean while making it a nutrient desert (Schlarbaum, 2008).The upper layer is nutrient depleted. This coincides with photosynthesis in the photic zone, which is the depth where photosynthesis available radiation is 1% of its surface value, and the consumption of nutrients necessary for the process (Pacciaroni & Crispi, 2007). The nutrient depleted surface is separated from a nutrient abundant layer, and a sharp gradient in nutrients which increases with depth. The availability of nutrients is strongly dependent on the thermal stratification of the water, known as thermocline, a barrier to diffusion of nutrient known as the nutricline, and the physical mixing of the water column (Cermeno et al., 2008).

Since deep water exchange in Gibraltar is blocked by a physical constraint imposed by the sill topography, as seen in Figure 6, only surface water, lower in nutrients, flows into the Western basin. The sill topography acts as a physical barrier and allows only the inflow of surface water, lower in nutrients, into the Basin. A second sill found in the Straits of Sicily separates the Western basin from the Eastern. Once again, the sill allows an inflow of surface water, lower in nutrients, into the Eastern basin, and an outflow of intermediate water, higher in nutrients into the Western basin. Both physical constraints block deeper water, rich in nutrients from flowing into the Mediterranean, while causing a significant nutrient decrease in the eastern basin.

The physical structure and the typical circulation make the Eastern Mediterranean Ultra-Oligotrophic, a trophic state characterized by low primary production in which chlorophyll concentrations fall lower than oligotrophic seas as a result of low nutrient content (Kenneth et

al., 2003; Yacobi et al., 1995). The deep blue color of the sea is an expression of the nutrient desert and low primary production, characteristics that assist in detection of abnormalities with evident change in color.

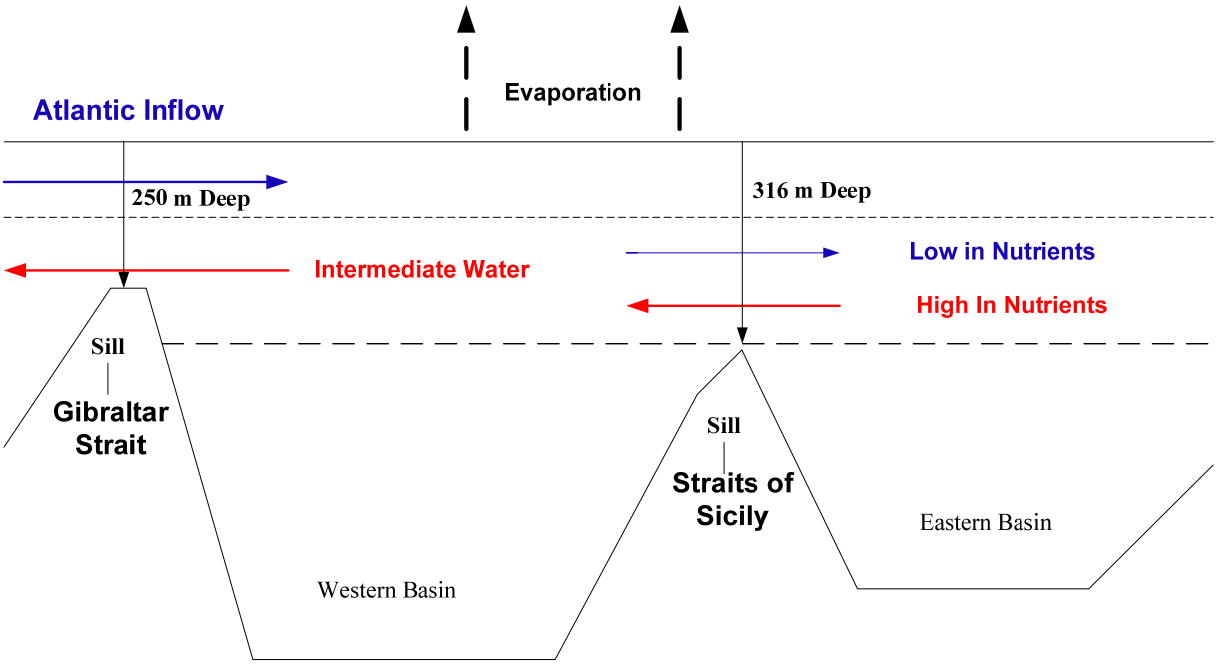

Figure 6: Circulation, and Water Exchange between the Eastern and the Western Basins

Source: Sinaya Dayan, 08/01/09

The general circulation in the Eastern basin is counterclockwise. It is an east to west flow offshore Sinai, gradually switching to a north-south flow along the Israeli coast. The Nile littoral cell, one of the largest in the world, spans a 650 km along the southeastern Mediterranean, from Abu Quir, Egypt, to Haifa Bay, Israel, and is the primary source of sediment to the southeastern Mediterranean, where alongshore currents are thought to be a driving force in the sediment transport within the cell (Carmel et al., 1984; Zvieli et al., 2007). The average Longshore Sand Transport, illustrated in Figure 7, decreases as it travels north, and diminishes at the Carmel coast just before reaching Haifa Bay. The amount of sediment transported had been significantly

reduced due to the construction of two dams in Aswan, Egypt (Klein et al., 2007; Perlin & Kit, 1999).

The typical sediment transport in the region determines the level of optically active constituents in Haifa Bay, and more importantly, to what extent the productivity, assessed by

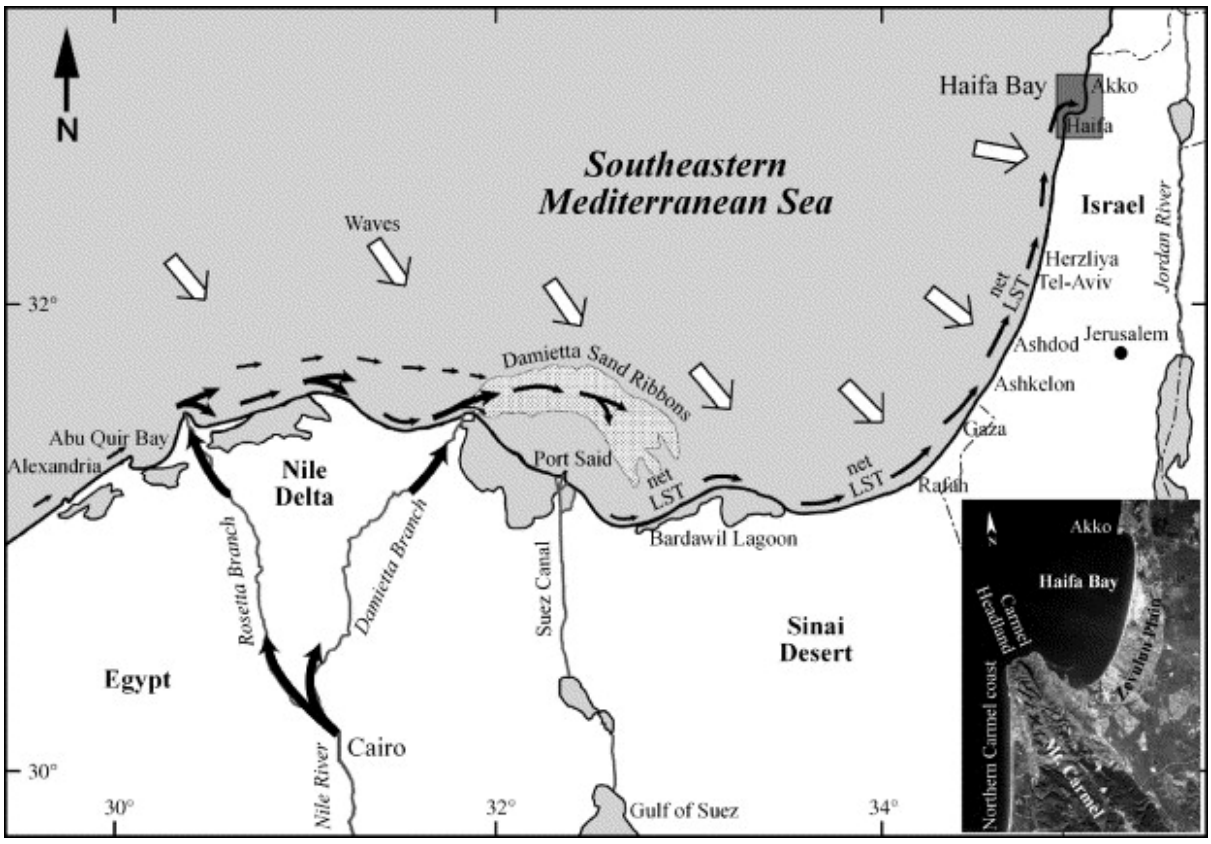

Figure 7: Longshore Sand Transport and ETM satellite image insert of Haifa Bay, Israel. Source: Zvieli et al, 2007.

chlorophyll concentrations, of the bay could be evaluated accurately with little interference from other constituents. Gitelson et al. (2000) corroborated this assumption and reported that non-organic suspended matter was very low in Haifa Bay, and that phytoplankton was responsible for over 90% of dry weight. Phytoplankton is considered the dominant constituent that determines the optical properties of the water in the region, with little optical influence or masking by sediments, suspended solids or particulates.

Marine Pollution & Eutrophication: Geospatial Analysis

By definition, "Marine pollution is the introduction by man, directly or indirectly, of substances or energy to the marine environment resulting in deleterious effects such as: hazards to human health, hindrance of marine activities, including fishing; impairment of the quality for the use of seawater; and reduction for amenities" (Hassan, 2005).

There are two categories of pollution: Point Source and Nonpoint Source. The U.S Environmental Protection Agency defines Point Source pollution as "any single identifiable source of pollution from which pollutants are discharged, such as a pipe, ditch, ship or factory smokestack" (Hill, 2004). Pollutants in this case are discharged into the river from a discrete point, such as municipal waste water, industrial waste water, power plants, etc. Non Point Source pollution, usually transported in surface water, diffuses at different intermittent levels and infiltrates the receiving medium (Jha et al., 2007). The extent of the pollution is closely linked with the runoff volume and velocity, which is dependent upon the characteristics of the basin, the soil permeability, hydrological parameters, precipitation, and landcover/landuse conditions. Runoff patterns are influenced both by climatic changes and seasonal properties, as they both affect flow rates as well as define specific conditions that shape the rainfall/runoff relationship. Runoff ultimately transports pollutants in the form of nutrients into marine ecosystems (Hessen et al., 1997).

As Orr (2008) documented, for a given amount of precipitation, increase in surface runoff is the result of increase in impervious surfaces with little friction, which generate higher volume and velocity. Changes in landcover, particularly urbanization and agriculture, increase the sheet wash that erodes the soil, and transports pollutants such as nutrients into aquatic and marine

environments (Fitzpatrick et al., 1999). Both agriculture and urban areas are considered major sources of nitrogen and phosphorous, which cause diverse problems that degrade the ecosystem, impair the quality of the water and intensify eutrophication (Carpenter et al., 1998). The task of detecting marine pollutants is usually done indirectly by monitoring the proliferation of biota and flora. The method assumes that proliferation of biota and flora is the result of the interaction with pollutants or materials. The detection then becomes possible since the inherent optical properties of biota and flora have unique spectral characteristics (Gitelson et al., 1996). This research uses a similar approach to detect marine pollutants as nitrates and phosphates by detecting the presence of algae. Since the active pigment, Chlorophyll, has a distinct spectral signature, it is relatively easy to detect remotely using many of the available commercial sensor systems.

Nixon (1995) defined eutrophication as the increase in the rate of supply of organic matter to an ecosystem. It is a normal aging process that affects all water bodies, though alteration of nutrient dynamics has dramatically intensified the process. Eutrophication of coastal waters is attributed to increasing population densities around the coastal zone. Prominent modes of human activities such as land clearing, agriculture, urban and industrial development, and other man derived activities introduced elevated levels of terrestrial inputs into marine environments (Cloern, 2001; Grall & Chauvaud, 2001; Nixon, 1995). Although many factors may increase the productivity of coastal waters, it is thought that a common single cause is nutrient enrichment such as nitrogen and phosphorous (Karydis & Chatzichristofas, 2003). Pearl and Whitall (1999) estimated nitrogen flux from different sources and concluded that about 40% comes from atmospheric deposition, 30% from riverine discharge, 10% from groundwater, and 20% from biological nitrogen fixation. Krom et al. (2004) as well as Herut et al. (2002) argued that the main source of nitrogen is anthropogenic, with increased flux from vehicle emissions,

agriculture growth, urban runoff, and industrial emissions. The relative contribution of atmospheric deposition to coastal waters is likely to increase drastically in the next decade, and impact coastal primary production, eutrophication, and phytoplankton community structure (Pearl, 1997).

Ecological indicators allow synoptic monitoring of water quality by factoring a range of environmental indicators into a single value by which the trophic state is determined. The appropriate model essentially assesses the water quality, and establishes quality objectives for a given environment (Giovanardi & Vollenweider, 2004). Nixon (1995) proposed a classification method for marine systems based on primary production measured as carbon concentration per square meter per year (Table 1).

Trophic State	Carbon Concentration ($Cm^{-2}y^{-1}$)
Oligotrophic	< 100 g
Mesotrophic	100-300 g
Eutrophic	301-500 g
Hypertrophic	>500 g

Table 1: Classification of Marine Environments: The classification is based on primary production and is measured as Carbon

Source: Nixon, 1995

Primary production is also measured as chlorophyll *a* concentration, often used as a representative parameter of marine eutrophication (Table 2) (Michelakaki & Kitsiou, 2005).

Trophic State	Chlorophyll *a* Concentration (mg/m^3)
Oligotrophic	0-0.084
Lower- Mesotrophic	0.084-0.359
Upper – Mesotrophic	0.359-0.793
Eutrophic	>0.793

Table 2: Classification of Marine Environments: The classification is based on primary production and is measured as chlorophyll concentration

Source: Michelakaki & Kitsiou, 2005

Oligotrophic areas are characterized with low nutrients, nitrates and phosphate, and low primary production. Mesotrophic areas are areas enriched with nutrients and have an intermediate level of productivity, whereas eutrophic water is rich in nutrients and algal biomass.

A more simplistic classification of ocean water divides it into two classes, case-1 and case-2 water, where the optical properties, absorption and reflection, of case-1waters are determined primarily by phytoplankton and other related Colored Dissolved Organic Matter. In case 2 water, the dominant substances are inorganic particles such as mineral particles (Mobley et al., 2004).

Ocean Color Geospatial Characteristics by Remote Sensing

Ocean color remote sensing technology is used in the aquatic and oceanographic monitoring effort as an indicator of ocean health. It provides essential tools and unique methods with which water quality is assessed remotely. This approach establishes a link between the physical and biological properties in marine and oceanic environments (Sathyendranath et al., 1991). The method rests on the use of spectral channels that provide radiometric information, and spectral variation in the water leaving radiance (Morel & Gentili, 2009). At the core of remote sensing of ocean color lies the idea that upwelling light, recorded by the sensors, is modified by the presence of water constituents. It illustrates the interaction between light, water, and water constituents, where alterations of spectral properties occur by absorption, reflection, or scattering of light by dissolved or suspended compounds (Kirk, 1994).

The optical properties, such as absorption, reflection, and scattering of water bodies are influenced by their content, which in turn affect the apparent color of the water. Main components affecting the color are phytoplankton, inorganic suspended material, and color dissolved organic matter, also known as yellow substance. Yellow substance is found primarily when detrital material

decay and release tannins into the water column; it is a product of decomposition of organic matter, mainly attributed to decomposition of phytoplankton (Sudarshana, 1985). The cell breakdown and release of tannins are responsible for a yellow color of the water, which is the optically measurable component. It absorbs the shorter wavelengths of light of the spectrum smaller than 400 nm, with strong absorption in the ultraviolet and maximum absorption at 450 nm in the blue.

Phytoplankton is a microscopic, free floating organism found in the illuminated surface layers of the ocean. The concentration of the main phytoplankton pigment, chlorophyll, is often used as an index for assessing phytoplankton biomass. The relationship between ocean color and chlorophyll concentration is influenced by the physical properties of phytoplankton communities such as pigment composition, pigment concentration, and cell size (Sathyendranath, Prieur & Morel, 1989). Remote sensing of chlorophyll has been successful in case-1 water, where optical properties are affected primarily by phytoplankton. In case-2 water like coastal water, the technique is far more complex, as the optical properties are determined by other materials which mask the presence of chlorophyll and its optical signature (Purkis, 2004).

Inorganic suspended materials include bottom sediments suspended by wave action and currents. Various other sources include upland agriculture crop erosion, terrestrial runoff, and shoreline erosion (Jensen, 2007).

Physical processes related to the interaction between light, water, and water constituents determine the nature of upwelling irradiance recorded by satellite sensors. The inherent color of the ocean is described by the reflectance ratio:

(Eq. 1) $R(\lambda) = E_u(\lambda)/E_d(\lambda)$

Where $R(\lambda)$ is the reflection ratio, $E_u(\lambda)$ is the upwelling irradiance and $E_d(\lambda)$ is the downwelling irradiance (Morel & Prieur, 1977; Morel & Gordon, 1980).Two main inherent optical properties are the absorption coefficient (a) and scattering coefficient (b), which determine the exponential

decay rate of the radiation flux per unit length. The combined action of scattering and absorption of light progressively diminish the amount of light that propagates through the water column. The process is termed light attenuation. The degree of attenuation is wavelength dependent and is determined by pure water characteristics and constituents within the water column (Purkis, 2004). In shorter wavelength, upper middle ultra-violet to middle green, 350-550 nm, attenuation is low and governed by the water constituents, particularly dissolved organic matter, which greatly increases absorption. In longer wavelengths, >600nm, attenuation increases rapidly and is dominated by absorption characteristics of pure water rather than water constituents (Purkis, 2004).

The nature and magnitude of absorption and scattering are dependent upon the bulk optical properties of the marine medium, which in turn is affected by the specific absorption and scattering coefficients of each of the water constituents. This relationship directly links between optical properties of pure water and its composition making it possible to remotely detect, quantify, and discriminate between water constituents based on their specific absorption and scattering coefficients (Bukata et al., 1995).

Essentially, remote detection of oceanic phytoplankton is achieved through the specific absorption and scattering coefficients of chlorophyll. Though numerical values fall into a broad range, as they are dependent on the phytoplankton population and physiological state, chlorophyll has several distinct effects on the reflectance spectra in the range from 500 nm to 700 nm (Gitelson et al., 2000). Gitelson et al. (1996) described a prominent wide minimum in the reflection values in the blue region of the spectrum, ranging from 420 to 500 nm (A), which corresponds with chlorophyll absorption. Their research also reported a reflectance peak in the green range near the 550-570 nm (B), a drop in reflection near 625 nm and at 670-680 nm (C, D)

and a narrow range peak near the 700 nm (E), possibly due to chlorophyll fluorescence (Figure 8). The maximum peak reflectance, as seen in Figure 8, in the green range around 570 nm, region B, was the result of minimum absorption of all algal pigments. Reflectance beyond the 750 nm depends on both inorganic and organic suspended matter and is insensitive to algal pigments. The most germane approach in measuring chlorophyll-a concentration remotely has been the use of reflectance ratios of the blue and green spectral channels (Gitelson et al., 2000).

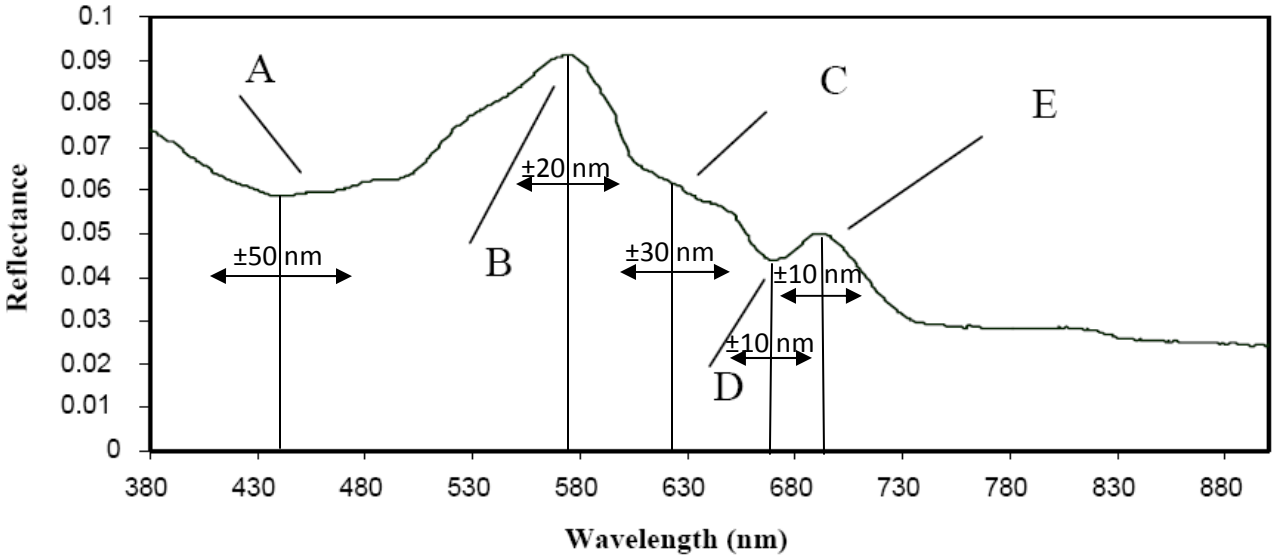

Figure 8: Reflection Spectrum of Haifa Bay waters with chlorophyll

Source: Adapted from Gitelson et al., 2000

Empirical algorithms are simple and have several advantages, as they can be derived from a limited number of measurements, they can be tested and implemented easily. They utilize simple statistical regressions of surface reflection against *in situ* measurements of water constituents, and are, therefore, widely used in ocean color remote sensing. O'Reilly et al. (1998) described a number of bio-optical algorithms, used to estimate the concentration of chlorophyll from ocean radiance. The algorithms described by O'Reilly et al. (1998) were tested on data recorded by the SeaWiFS sensor, but are applicable to other sensors with similar spectral channels. The majority of algorithms utilize the reflectance ratio R443/R550, when chlorophyll concentration falls

below 1.5 mg/m^3. The reflectance ratio R520/R550 is used when chlorophyll concentration > 1.5 mg/m^3.

In oligotrophic waters chlorophyll concentration is determined by using the following algorithm:

(Eq. 2) Chlorophyll-a (mg/m^3) = a $(R_{443}/R_{550})^{-b}$.

R_{443} and R_{550} represent the recorded reflectance values in their corresponding spectral channels ± 10 nm, while the parameters *a* and *b* are the absorption and scattering coefficients, which are unique to each water body (Iluz et al, 2003). Gitelson et al. (1996) assessed the accuracy of algorithms and coefficients values described in several research projects. Since coefficient values, used in prior studies, yielded a significant error both for low chlorophyll concentration, as well as for high chlorophyll concentration, a modified algorithm was adapted for the Southeastern Mediterranean:

(Eq. 3) Chlorophyll-a (mg/m^3) = 0.914 $(R_{440}/R_{550})^{-1.86}$

The modified algorithm utilizes similar spectral channels as described in earlier studies, it however, uses specific, more accurate coefficients value. Estimation of chlorophyll concentration in Haifa Bay utilizes the same algorithm, as it assumes that coefficients for the Southeastern Mediterranean are representative of the bay waters.

Statement of Research Problem and Proposed Solution

For more than a decade, the Israel Oceanography & Limnology Research group has monitored the quality of the coastal waters of Israel to provide a scientific basis for the development of environmental protection policies. Such policies allow effective enforcement of regulations, assure law compliance, and enable the development of strategies that promote the protection of nature. The objective is to create a platform that mitigates, and prevents the

deterioration of the marine ecosystem, with the emphasis on identifying the underlying processes that affect the health of the marine environment, particularly areas subjected to extreme anthropogenic pressure like Haifa Bay.

The data collected by Israel Oceanography & Limnology Research group revealed that the water in Haifa Bay show elevated levels of nutrients not typical to the Southern Mediterranean waters, which are ultra oligotrophic, (see Figure 9). Nutrient enrichment contributes to increase in primary production, measured as chlorophyll concentration, which is especially evident in the bay waters (Figure 10). In productive water the secchi depth is low compared with non productive areas, where water achieves high secchi depth and the disc used to measure water clarity is seen to greater depths (see Figure 11). The measurements are used to monitor the marine environment, as well as to shorten the response time when conditions worsen.

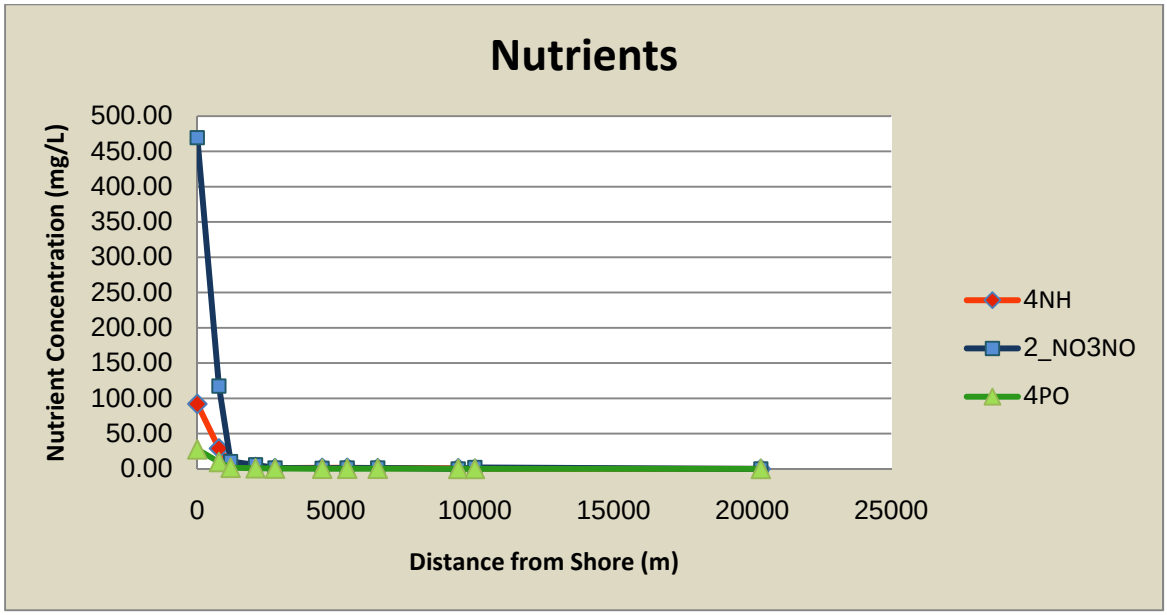

Figure 9: Nutrients Concentration in Haifa Bay as a Function of the Distance from Shore

Source: Sinaya Dayan, 08/01/09

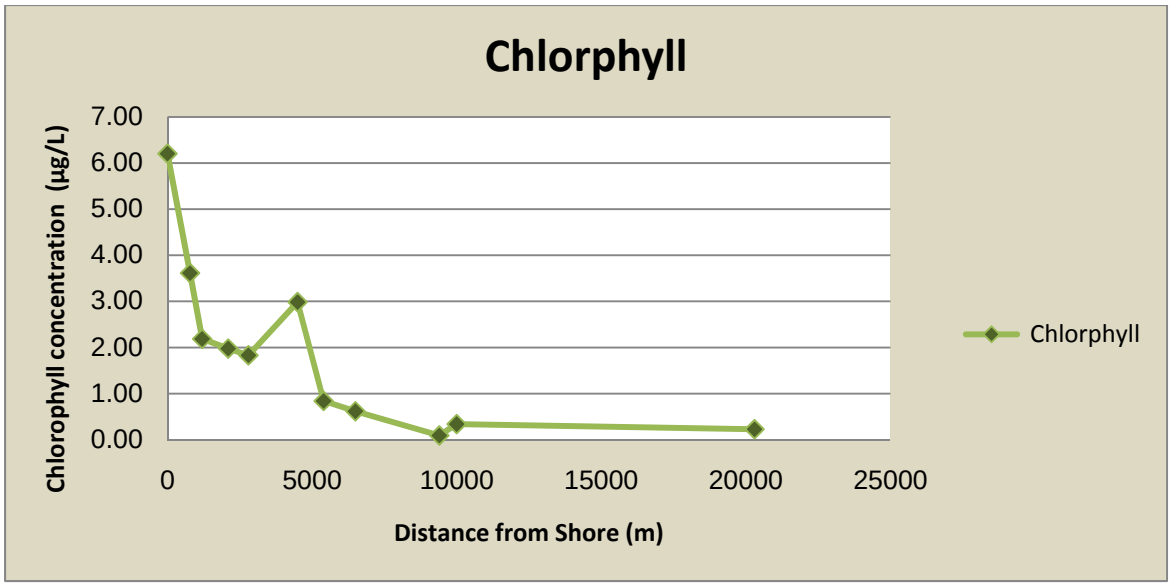

Figure 10: Chlorophyll Concentration in Haifa Bay as a function of the Distance from Shore

Source: Sinaya Dayan, 08/01/09

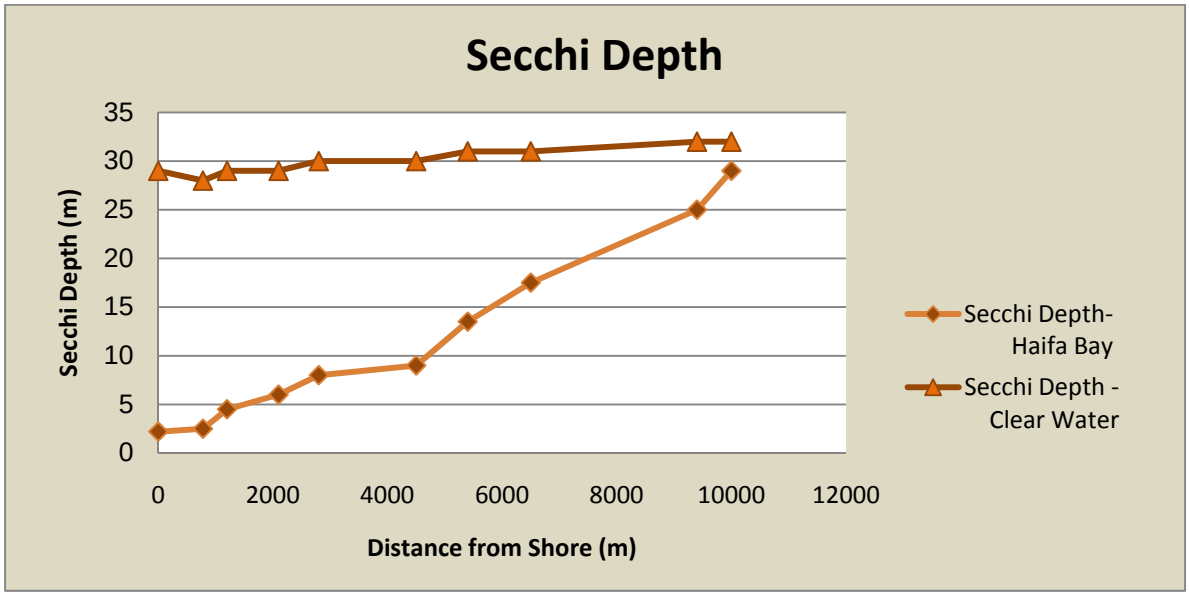

Figure 11: Secchi Depth in Haifa Bay as a Function of the Distance from Shore

Source: Sinaya Dayan, 08/01/09

The majority of the coastal waters in Israel are enriched with nutrients and show elevated levels of chlorophyll. The common method of using *in situ* measurements to quantify the levels of chlorophyll and to identify sources that contribute to this phenomenon is an adequate but time consuming and costly option. This research *problem* is to demonstrate the advantages of using a more practical and effective alternative to the common monitoring challenges. Remote sensing technology makes it possible to observe events in remote and inaccessible areas, enables frequent sampling and provides a source for synoptic data. The *proposed solutions* of this research are to create a terrestrial geobiophysical model to show sources for increases level of nutrients, and to create marine geobiophysical models to validate algorithms for the geospatial assessment of chlorophyll concentration, through the calibration of remote sensing spectral channels to *in situ* measurements.

CHAPTER II

Research Methods and Techniques

Geospatial Research Area for Geobiophysical Modeling

Haifa Bay, approximately 18 kilometers long, is the only natural harbor in the coast of Israel (Figure 12), and is the largest of the commercial ports operating in the state. The Bay is the most significant morphological feature on the Southeastern Mediterranean coast. It opens to the west and is bordered by the Carmel Mountain to the south, Zevulun plain to the east, and the city of Acre to the north. The bay area hosts a bustling industrial zone, and is a significant metropolitan area in the state (Zviely et al., 2007). Elevation ranges from 41 m above sea level in the Jezreel plain to 548 m above sea level in Mount Carmel (Figure 13). The soil within the Kishon watershed consists mainly of gravel, sand, and clay (Figure 14). The texture of the alluvial soils is sandy clay with 46.8%,

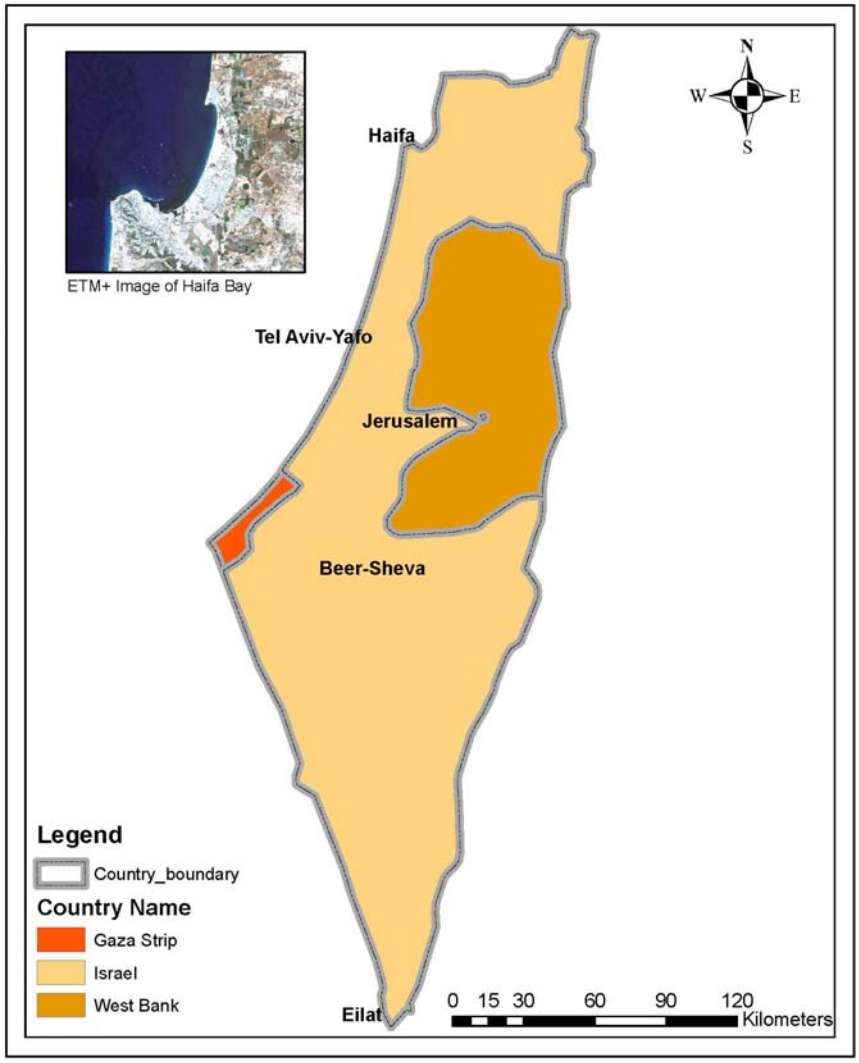

Figure 12: Map of Israel and the Study Area

Source: Sinaya Dayan, 08/01/09

12.4%, and 40.7% of clay, silt, and sand, respectively. This soil type has a good natural drainage system, is excellently suitable for irrigated crops, and is, therefore, the most intensively cultivated soil in Israel (Singer, 2007).

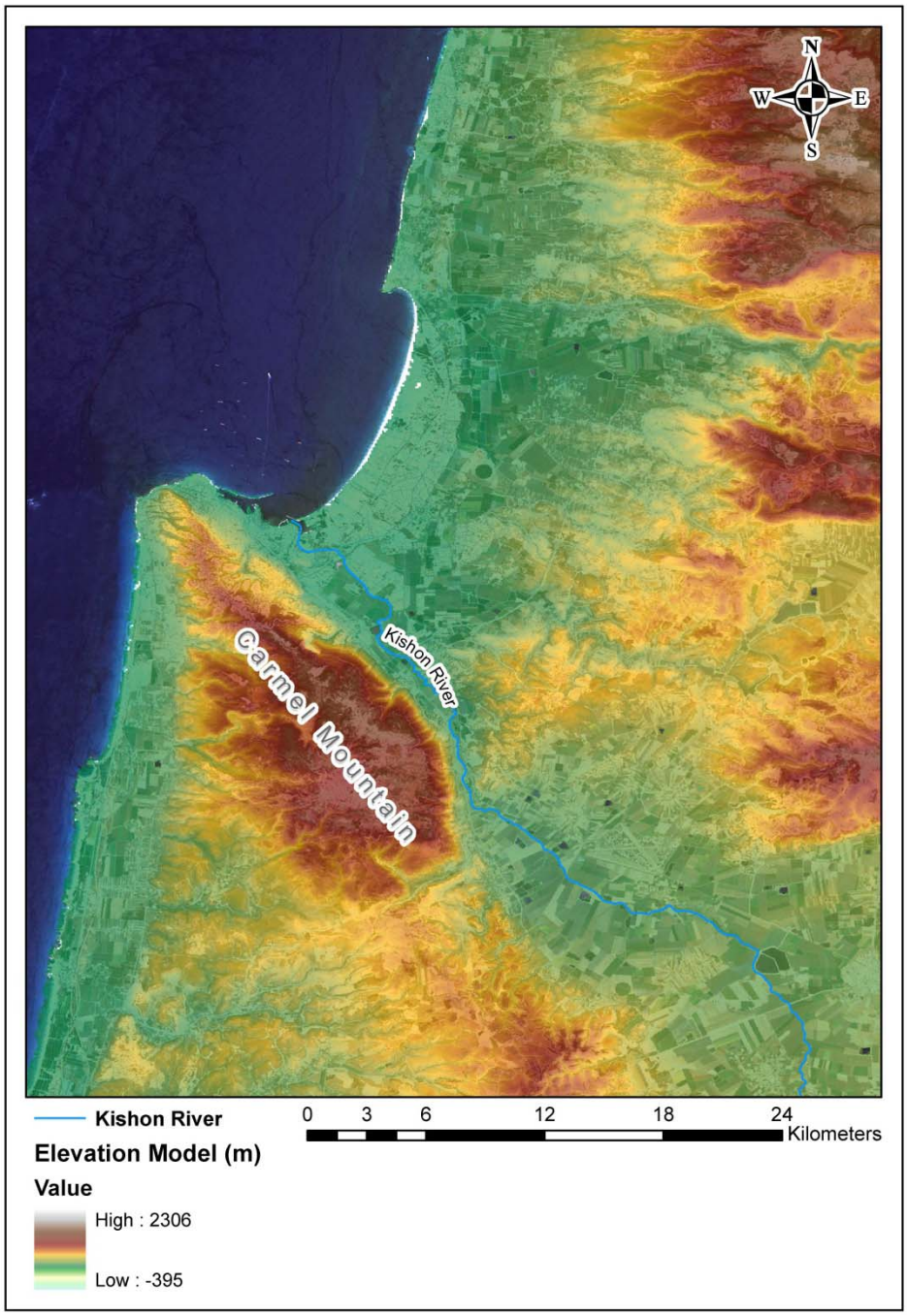

Figure 13: Elevation Model of the Bay Area, ETM+ May 21 2000

Source: Sinaya Dayan, 08/01/09

Figure 14: Soil Map of the Bay and Surrounding Areas, ETM+ May 21 2000

Source: Sinaya Dayan, 08/01/09

The model includes both terrestrial as well as marine areas, and accounts for the interaction between the two environments. As terrestrial inputs make their way into the coastal waters, it was eminent to incorporate a terrestrial model into the research, and assess its influence

on the marine environment. Essentially, the immediate study area included both a buffer of 20 km around the Kishon River for the terrestrial component of the geobiophysical model, as well as the Haifa Bay waters for the marine component of the model.

Remote Sensing and In Situ Data Acquisition for Geospatial Analysis and Modeling

Advancements in remote sensing technology provide unique methods of assessing land use and land cover, mapping, and monitoring projects. For thematic representation and terrestrial assessment, this study used raster image data collected by Landsat 7 Enhanced Thematic Mapper sensor, ETM+. For ocean color purposes, datasets from ETM+ and Medium-Spectral Resolution, Imaging Spectrometer, MERIS were used. ETM+ records the earth's surface with 30 meter spatial resolution in six spectral bands, visible through near infra red, 15 m in one panchromatic band, and 60 m in one thermal band, a total of 8 bands. The multispectral scanning radiometer detects and records radiation in the visible near infrared, short-wavelength infrared, and long-wavelength infrared, regions (Table 3) (NASA, 2009).

Band Number	Wavelength (µm)	Spatial Resolution
TM1	0.45-0.515	30 m
TM2	0.525-0.605	30 m
TM3	0.63-0.69	30 m
TM4	0.75-0.90	30 m
TM5	1.55-1.75	30 m
TM6	10.4-12.5	60 m
TM7	2.09-2.35	30 m
TM8	0.52-0.9	15 m

Table 3: ETM+ Band Description

Source: NASA, 2009

This research utilized two different ETM+ datasets, each with a distinctive purpose. The first was acquired on May 21 2000 and was primarily used for land use/ land cover classification,

and later in the creation of a runoff model. A second ETM+ dataset was acquired on August 25, 2000 and was suitable for chlorophyll detection, as *in situ* measurements from August 27, 2000, were available and could be integrated into specific chlorophyll algorithms.

The use of satellite images in ocean color research made a significant contribution in oceanographic research since the launch of the Coastal Zone Color Scanner (CZCS) in 1978 (Aiken et al., 1992). Since then, other ocean color sensors (SeaWiFS, MOS, OCTS, etc.) were launched, making data more accessible and readily available to end users. Of specific interest to this study is the Medium-Spectral Resolution Imaging Spectrometer. The MERIS sensor is onboard of the ENVISAT satellite, which offers a continuous, global observation of the oceans for enhanced ocean modeling. The ENVISAT satellite of the European Space Agency was launched in 2002, and is the largest earth observation space craft ever built. It was launched into a sun synchronous polar orbit at an altitude of about 800 km. The satellite orbits the earth in 101 minutes and provides a complete coverage of the globe every three days. Its optical instruments provide continuous observation and monitoring of land, atmosphere, ocean and ice caps (ESA, 2009). The MERIS imaging spectrometer is a push broom sensor with linear arrays of Charge Coupled Devices that provide spatial sampling in the across-track direction, while scanning in the along-track direction is provided by the satellite motion, (see Figure 15). The instrument's instantaneous field of view is divided into five segments, each of which is imaged by one of the corresponding sensors covers a swath width of 1150 km, centered around the sub-satellite point. The sensor records reflected solar radiation in 15 spectral channels selectable across the 390-1040 nm range, which are programmable in position and width, see Table 4 for bands description (ESA, 2009).

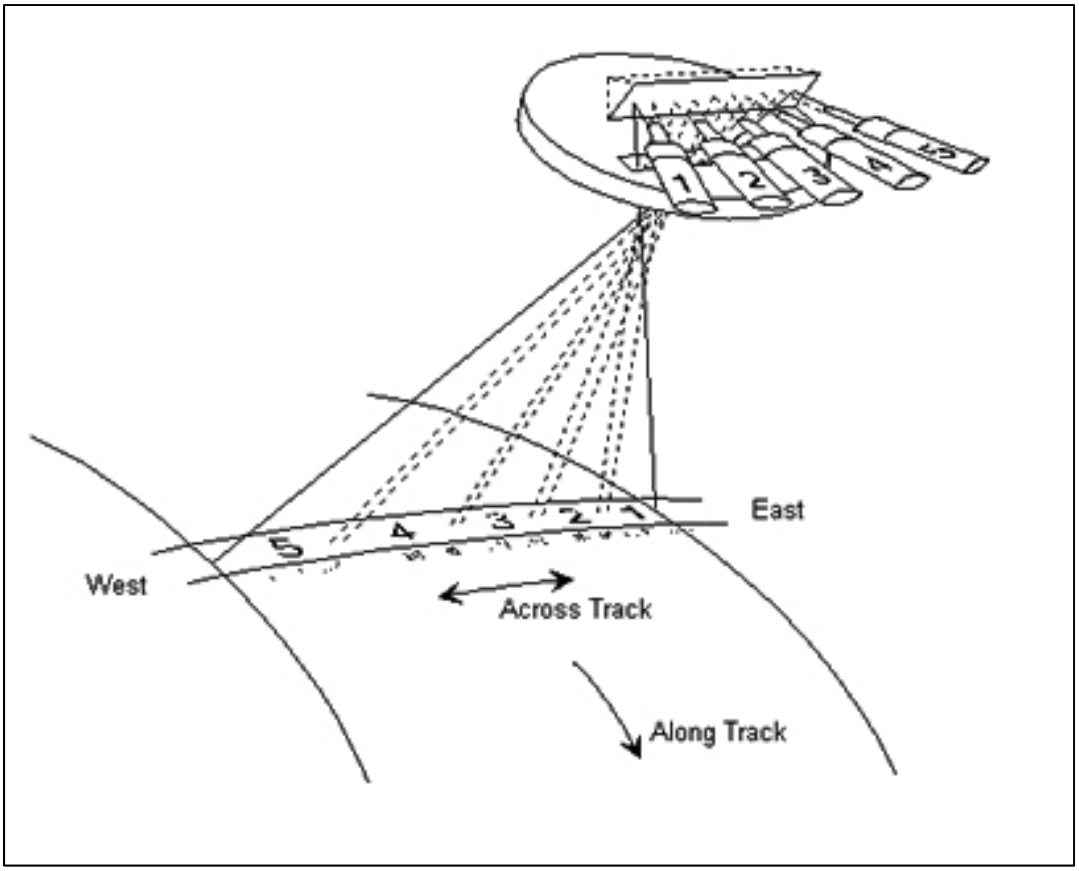

Figure 15: MERIS IFOV, Satellite and Cameras Tracks

Source: ESA, 2009

Band Nr.	Band center (nm)	Bandwidth (nm)
1	412.5	10
2	442.5	10
3	490	10
4	510	10
5	560	10
6	620	10
7	665	10
8	681.25	7.5
9	705	10
10	753.75	7.5
11	760	2.5
12	775	15
13	865	20
14	890	10
15	900	10

Table 4: MERIS Bands Description

Source: ESA, 2009

As availability of products is dependent upon the geographic location and times of collection, full resolution products, although preferred, are not always available. As in the case of this study, *in situ* measurements determined the specific date of the raster dataset to be used. Since *in situ* measurements were taken on March 22-24 2004, the study required that MERIS datasets were from the same time period. A dataset from March 23 2004, was found most suitable, and as a result was used for further processing. On this specific date, only reduced resolution products were available resulting in 1200 m spatial resolution

In situ Measurements for Geospatial Analysis and Modeling

According to Kress & Herut (1998) nutrient concentrations in the bay remain constant during all seasons. Chlorophyll concentrations, on the other hand, vary seasonally, with lowest concentration during the winter when productivity is inhibited by low temperatures, and highest concentrations during spring when conditions are ideal. Although the localized influence close to the estuary was elevated, it diminished drastically seaward to normal oligotrophic conditions (Kress & Herut, 1998).

In situ measurements of Haifa Bay water constituents for this research were available through the Israel Oceanography & Limnology Research Institute, which provided the data for this research. Data were collected on two separate occasions: August 27, 2000, and March 22-24, 2004. Of specific interest were chlorophyll measurements of surface waters in Haifa Bay. On August 27 2000, 8 stations were sampled and several water quality parameters were tested. This study, however, focused solely on Chlorophyll concentrations, which are presented in Table 5. The spatial distribution of the sampled station is presented in Figure 16.Similarly, On March 22-24, 2004, 11 stations were sampled linearly where chlorophyll concentrations were measured.

Chlorophyll concentrations at each station are presented in Table 6, while spatial distribution of sampled stations are presented in Figure 17.

Station	Chlorophyll a mg/l
c1	4.65
c2	11.4
c3	5.95
c4	0.3675
c5	0.4
c6	0.6925
c7	0.28
c8	0.289

Table 5: *In Situ* Chlorophyll Measurements in Haifa Bay Israel, August 27, 2000

Source: Israel Oceanography & Limnology Research institute

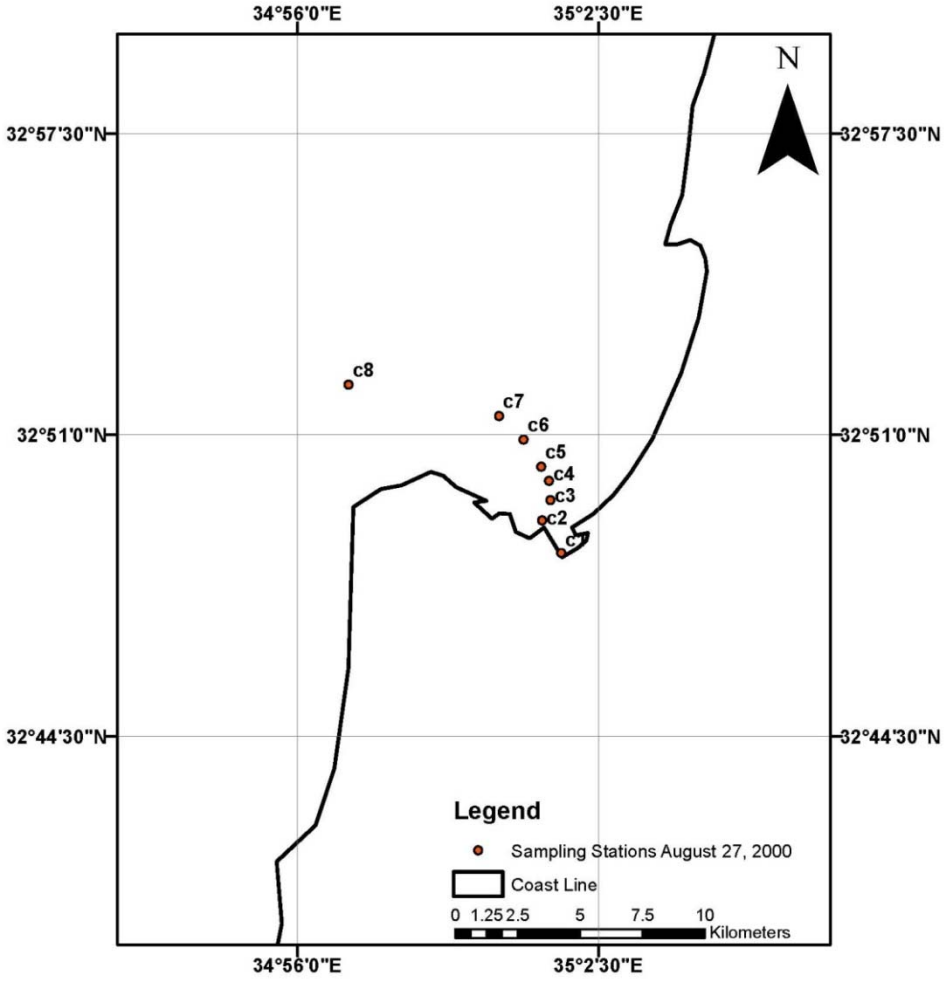

Figure 16: Map Display of the Sampling Stations in Haifa Bay, Israel, August 27, 2000.

Source: Sinaya Dayan, 08/01/09

Station	Chlorophyll a µg/l
St1	6.202
St2	3.613
St3	2.187
St4	1.977
St5	1.830
St6	2.984
St7	0.841
St8	0.617
St9	0.092
St10	0.339
St11	0.227

Table 6: *In Situ* Chlorophyll Measurements in Haifa Bay, Israel, March 22-24, 2004

Source: Israel Oceanography & Limnology Research institute

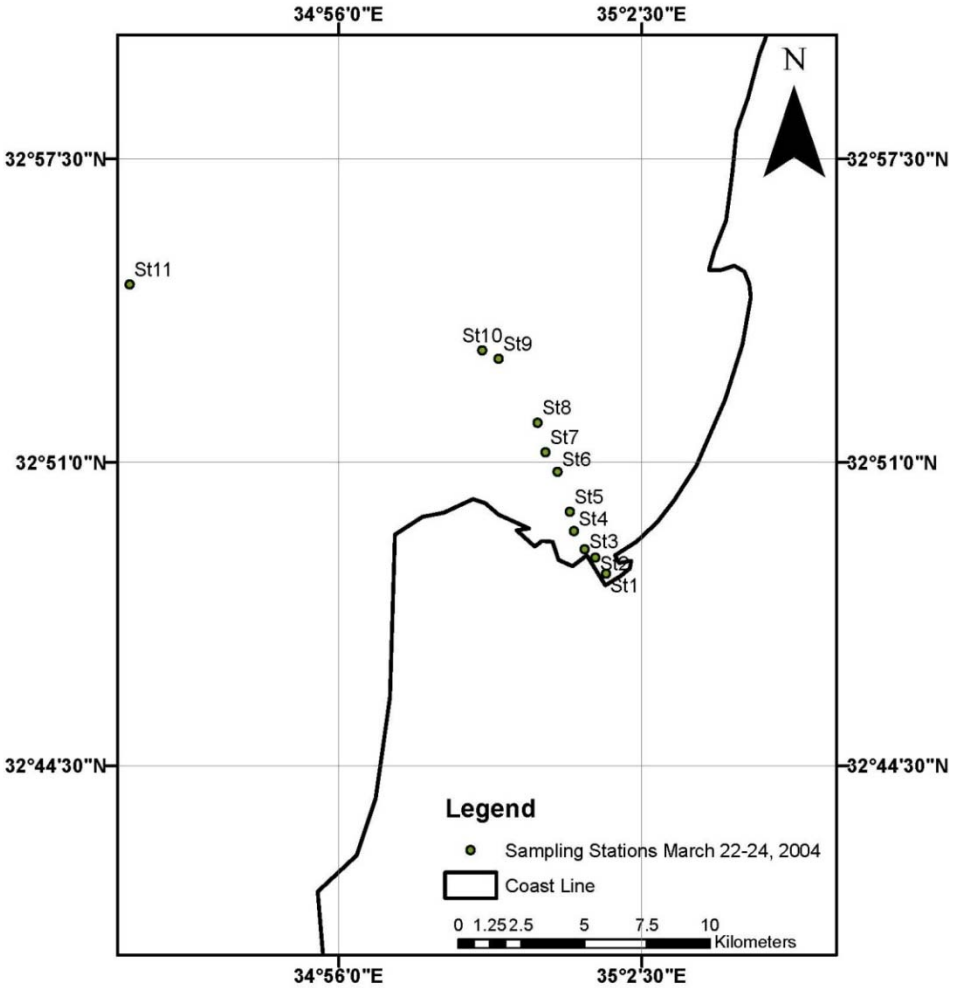

Figure 17: Map Display of the Sampling Stations in Haifa Bay, Israel, March 22-24, 2004

Source: Sinaya Dayan, 08/01/09

Image Processing Techniques for Geospatial Analysis and Modeling

ETM+ Image data were delivered as eight separate bands in a GeoTIFF, a widely used data file format. All raster datasets were geo-registered to the same coordinate system, UTM Zone 36N, making sure the data were aligned properly. Since the terrestrial area of interest was set to a buffer of 20 km around the Kishon River, as it is the main transporter of terrestrial inputs into the bay, each of the bands was clipped to the area of interest, using ESRI ArcGIS 9.3. This step ensured that the only the immediate environment, which was most relevant to the analysis was included in the model (Figure 18).

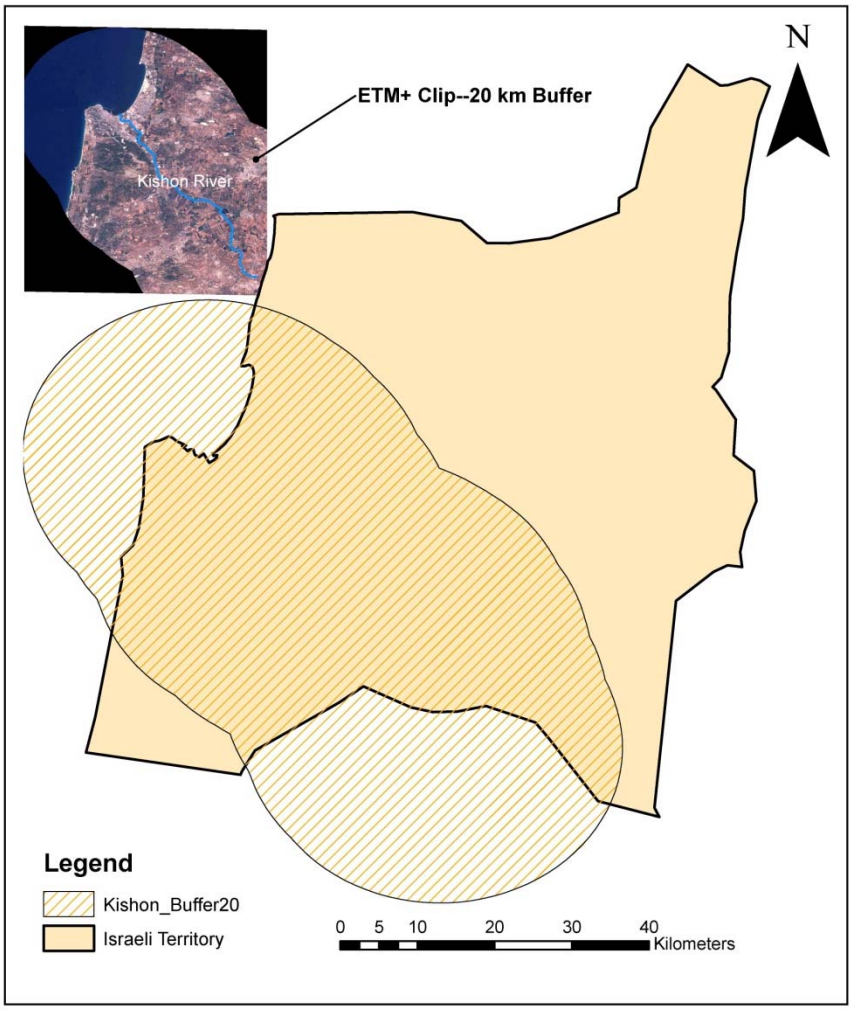

Figure 18: 20 km Buffer around the Kishon River & Haifa Bay, Israel.

Insert: ETM+ cropped image from May 21 2000 was used for land cover analysis and the creation of a runoff model.

Source: Sinaya Dayan, 08/01/09

After each band was clipped to the buffered area, the separate bands were compiled to create a multispectral image, allowing all bands to be displayed, processed and analyzed though a single multiband image file. Image compilation was done using ER Mapper 7.1. Similar processes were required in the ETM+ data of aquatic area of interest. In this case, each band was clipped to area containing only the Haifa bay water (Figure 19. Clipped individual bands were then complied to create a single multispectral or composite image file. Both terrestrial and aquatic inputs were used in further processing and analysis.

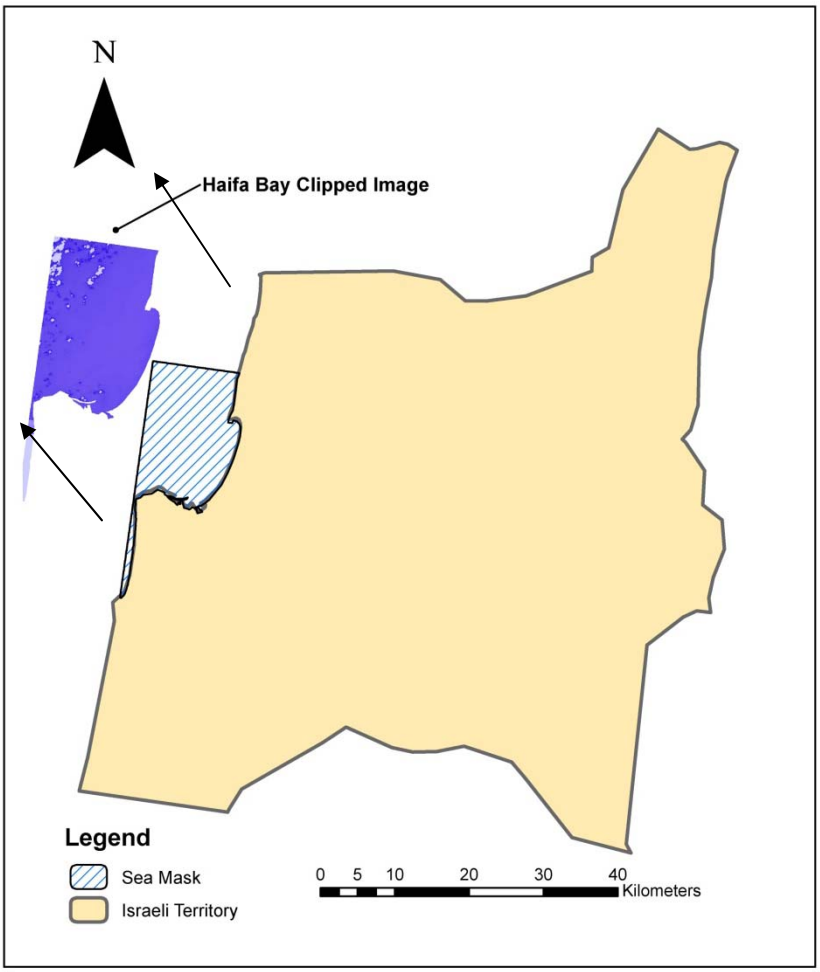

Figure 19: Clip of Haifa the Bay Waters, ETM+ August 27, 2000

Source: Sinaya Dayan, 08/01/09

MERIS image data were delivered in a hierarchical structure, which could have been processed only by using BEAM, a toolbox used for viewing, processing and analyzing raster data recorded by Envisat's electro-optical sensor instrument. Essentially, ESA's software package was used for viewing the data and for converting the typical hierarchical data structure to a GeoTIFF, which could then be accessible by ER Mapper 7.1, and ESRI ArcGIS 9.3. Once all preprocessing steps were finished, the data were ready for further processing which is discussed in the next chapter.

Geospatial Multivariate Classification Methods and Techniques

Feature extraction for pattern recognition aims to classify data based on knowledge or statistical features information extracted from patterns. The mechanism computes numeric, information, or features from the observation, and allows a close examination or analysis of patterns within data.

Clustering procedures are extremely effective for region analysis in feature extraction and pattern recognition, and are often a major task in image information processing. Methods of analysis combine spectral, spatial, and contextual clustering, which are essential for identification of patterns and extraction of features (Hugh et al., 1997). Multiband classes enable pattern recognition, and are derived statistically where each unknown pixel is assigned to a class using the appropriate method. Brumfield et al. (1997) demonstrated that landscape processes and characteristics produce predictable patterns essential to the understanding and the representation of ecological changes. Patterns within an image could be identified efficiently using remotely sensed data and cluster algorithms, to produce meaningful representations of the feature information captured in the imagery

Classification was performed using ISOCLASS, an unsupervised classification technique in ER Mapper. The ISOCLASS divides data into groups that are statistically meaningful. The goal of the cluster is to capture the natural structure of the data and group objects according to common characteristics (Gunther, 1981). The greater the similarity within a group, and the greater the separation of the group, the more distinct are the clusters and classification. The algorithm utilizes an iterative process that starts with calculated approximate means assigned by the software, one for each of the clusters. The process, comprised of several iterations, assigns every pixel in the imagery to the closest of arbitrary means in the mathematical multidimensional space. The algorithm then computes new means for each cluster based on the membership of pixels as determined by the prior iteration. Pixels are reassigned until a finite classification is achieved, and the process completes (Ball & Hall, 1965).

Classification techniques were performed exclusively on ETM+ data from May 21, 2000, as part of the terrestrial runoff modeling and the identification of sources responsible for nutrient enrichment in the bay water. It offered a possibility of exploring the structure of data without guidance in the form of class information, which can often reveal features not previously expected or known about. Utilizing the ISOCLASS unsupervised classification technique, a maximum number of classes of 10, 13, and 16 was set using multispectral bands one through five and seven. The thermal and panchromatic bands were excluded, as the thermal band measures the amount of infrared radiant flux, emitted from surfaces and is used for locating geothermal activities, urban heat sinks, and thermal plumes in water bodies. The panchromatic band is a grayscale image that covers the red, green, and blue portions of the electromagnetic spectrum and is used to improve the apparent spatial of resolution of multispectral bands. Setting different

class limits assisted in identifying the optimal number of classes, which best represented land features. Defaults were used for all settings but the maximum number of classes.

Principle Component Analysis, PCA, was also used in the classification process. The procedure reduces the number of dimensions by highlighting similarities and differences, and compressing the data with minimal loss of information. ER Mapper PCA algorithm uses each image band as a variable and transforms them to PCA components, where the first component accounts for the majority of variability in the data, and each succeeding component accounts for the remaining variability. In order to classify the original image using this procedure, PCA technique was applied on ETM+ bands one through five and seven to produce six outputs i.e., PC1, PC2, PC3, etc. PC1 through PC6 were then used as the input bands to generate a classified, thematic representation of land features.

Although accuracy assessment is important for analysis, performing such assessment was restricted due to lack of detailed ground control data availability. The current policy of the Israeli center for mapping, geodesy, cadaster and geoinformatics forbids the passing of geospatial information out of the State of Israel, preventing complete access to reference, ground truth, data required for the assessment. Regardless, the study relied on any available sources, including maps, online platforms i.e., Google Earth, Maps, ArcGIS Explorer, etc., literature, personal research knowledge of field data, and visual inspection of imagery to verify that land cover or land use features matched the classified image as accurately as possible. The accuracy of the classified image was a sufficient approximation for the modeling performed in this research.

The classified image data believed to be best was then integrated into a geographic information system, ArcMap 9.3, for the creation of a runoff model. The runoff model utilized the C factor or runoff factor, most commonly used in the rational equation, which is the simplest

method to determine peak discharge from drainage basin runoff (McCuen, 1998). Runoff values determine the erosive power, which is dependent upon a given land cover type contained within the hydrological system. The underlying assumption links runoff and sheet erosion to the method by which nutrients are introduced into the bay waters, where high values represent a potential source for increased introduction rate.

Suitable runoff coefficient values were added to the attribute table for each feature class of the classified image, and were determined according to the potential runoff of a given land cover (Hager, L.S, 2008; McCuen, 1998; Seidel & Martinec, 2004). Runoff is affected by the land surface, where impervious surfaces, bare earth, and agricultural activities provide increased runoff, and increased rate of introduction of nutrients. Deep sea and coastal area have no contribution and were, therefore, assigned the value zero. The river effluent/Mediterranean interface, on the other hand, would have the highest rate and was assigned the value 1.00. High intensity urban and industrial areas had a value of 0.85, while bare land had a value of 0.6. Agriculture activity ranged from 0.3-0.5 for plowed fields and cultivated rows, respectively. Mediterranean grove, the typical evergreen vegetation covering the Carmel Mountain, had value of 0.3, a runoff value affected mainly by the steep slope and vicinity to the bay. Evergreen vegetation had a value of 0.2, while light transitional vegetation had a value of 0.5, runoff thought to be rather significant due to decreasing resistance to overland flow. C values for each land cover were identified and determined based on earlier studies (Hager, L.S, 2008; McCuen, 1998; Seidel & Martinec, 2004) and are presented in Table 7.

Class Name	C Factor Value
Deep Sea	0
Coastal zone	0
Effluent/Mediterranean Interface	1.00
High intensity Urban/Industrial	0.85
Plowed Fields	0.5
Cultivated Agriculture Rows	0.3
Mediterranean Grove	0.3
Evergreen Vegetation	0.2
Light Vegetation	0.5
Bare Land	0.6

Table 7: Runoff Coefficient for Each Class.
Source: C values for different land covers were based on earlier studies by Hager, L.S, 2008; McCuen, 1998; Seidel & Martinec, 2004.

Applying thresholds on the runoff coefficient values identified suitable locations for increased levels of nutrients. Potential land classes, exhibiting favorable conditions for increased runoff and increased levels of nutrients, held a runoff coefficient greater or equal to 0.40. This value included agriculture activities, urban and industrial regions, bare earth and light vegetation areas. By applying a spatial condition using Map Algebra in ArcMap 9.3, it was possible to isolate regions that featured conditions of increased runoff. The spatial condition, referred to as **Con** function in ArcMap 9.3, controls the output value for each cell based on whether the cell value meets the specified conditional statement. The spatial condition employs the Boolean approach, which applies true or false values based on the information stored in each pixel. The syntax of **Con** function uses the generalized form:

(Eq. 4) **Con** (<condition>, <true_expression>, <false_expression>)

Con is the type of the conditional tool used for the spatial evaluation; <condition> is a conditional expression that is evaluated for each cell; <true_expression> is the value applied to

cells meeting the condition statement. Results that do not meet the condition statement are identified through the <false_expression>, which applies the false value to those cells.

Once potential regions were identified as true regions, meaning as regions which had a runoff coefficient equal or higher than 0.4, six spatial buffers were superimposed over the runoffs model containing such regions. The buffers were created using the buffer analyst in ArcMap 9.3, with which three areas of five, seven, and ten kilometers were buffered around the bay and three areas of two, five and seven kilometers were buffered around the Kishon River. By specifying distances around the bay and Kishon River it was possible to contain probable sources of nutrients and the relative impact of each of the buffered areas.

Band Ratioing and Ocean color Algorithms Applications to Geospatial Analysis and Modeling

Ratio technique is accomplished by dividing the data base brightness values in one spectral band by the data base BVs in second spectral band for each spatially registered pixel pair (Jensen, 2005). This study utilized the band ratioing technique in order to detect chlorophyll presence, as it is the most widely used method of estimating chlorophyll concentration in marine environments. The technique primarily uses the relative reflectance of blue and green, taking into account maximum absorbance of chlorophyll in the blue region and minimum absorbance by phytoplankton in the green (Gitelson et al., 1994; Mayo et al., 1995).

The study evaluated chlorophyll algorithms, through band rationing, by comparing *in situ* measurements of water constituents, chlorophyll concentration, to corresponding brightness values recorded both by ETM+ and MERIS sensors. The dynamic oceanic environment requires that *in situ* measurements and image datasets are collected during the same time period ± 2 days.

Timing is critical, as chlorophyll concentrations at the sampling sites fluctuate rapidly depending on currents, wave action, wind action, and other factors.

Tabular records, *in situ* measurements and coordinates for each sampling station, were converted to a point shape file. Displaying and overlaying the shape file provided a graphic illustration of the location from which samples were taken and their corresponding pixel (Figure 20, A). Using pixel inspector, reflectance values from each band of the relevant pixels were recorded and incorporated into the statistical regression models of both MERIS and ETM+ datasets (see Figure 20, B).

Figure 20, A: ETM+ August 25, 2000, Sampling stations in Haifa Bay, Israel correspond to the inspected pixels.
Source: Sinaya Dayan, 08/01/09

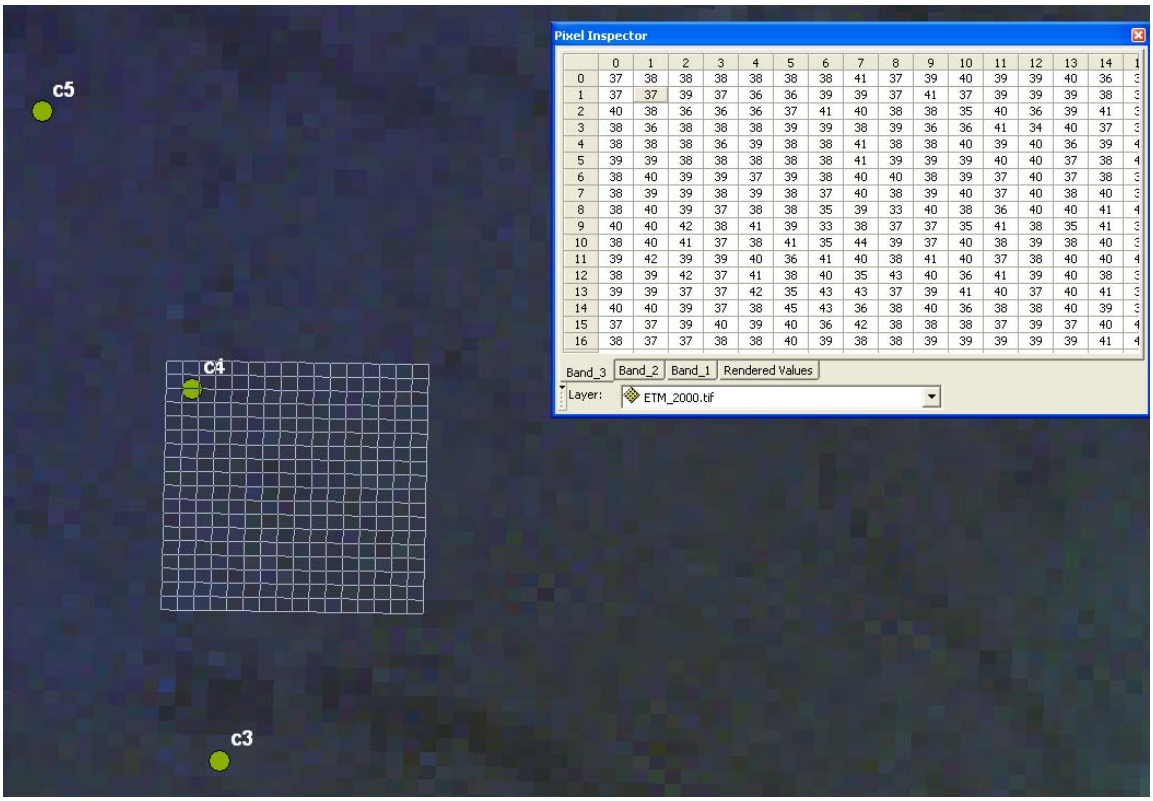

Figure 21, B: ArcMap 9.3 Pixel Inspector ETM+ August 25, 2000. The tool allows the inspection of reflectance values of the image pixels. Grid on the left represents the image pixels, while the table on the right displays brightness values at the inspected pixel and its surrounding cells. Inspected pixels correspond to the sampling stations in Haifa Bay, Israel. Source: Sinaya Dayan, 08/01/09

Of particular interest were reflectance values in the visible spectra from bio-optical algorithms, developed to estimate chlorophyll concentrations, incorporate spectral properties in the green and blue regions. Gitelson et al (1994) found that the Thematic Mapper, TM, algorithm (TM2-TM3)/TM1 is suitable for determining chlorophyll concentration at the low concentrations as found in this study. Mayo et al (1995) determined that reflectance in the region 620-690 nm (TM3) is dependent primarily on the concentration of suspended matter and could, therefore, be subtracted from the radiance in TM2 to correct for the additional radiance caused by scattering of non organic suspended matter.

Using MERIS radiance information, other algorithms, such as R443/R555, R520/R550 R490/R560, effectively estimate chlorophyll concentration, as spectral channels are tailored for remote sensing of water. Spectral reflectance at 443 nm, 490 nm, 520 nm, and 560 nm have been evaluated in simple ratio techniques, and proved to be successful in retrieving chlorophyll concentrations via remotely sensed data (Aiken et al., 1992; Gitelson et al, 1996; Iluz et al, 2003; Morel and Gentili, 2009; O'Reilly et al, 1998). These spectral channels are particularly useful since they record the optical response of phytoplankton within the spectral window, which highlights the spectral properties of the active pigment.

The algorithms were applied and tested using statistical regression models in order to determine the relationships between electromagnetic energies received by the different sensors and the desired oceanic parameter, in this case chlorophyll concentration. Similar algorithms were applied on the image dataset utilizing the appropriate spectral channels and band ratio techniques in ER Mapper. This technique allowed a visual inspection of the algorithm output, and offered a method of mapping the geospatial distribution of phytoplankton chlorophyll within the bay area.

CHAPTER III

Results and Discussion

Terrestrial Geobiophysical Model

The objective of the terrestrial geobiophysical model is to identify sources from which nutrients are transported to Haifa bay. Initially, the image dataset was processed to produce a set of classified images using various classification techniques. Post classification and selection of best classified imagery, a runoff coefficient was added to the attribute table of the classified image, based on the runoff potential of the different land categories. Ultimately, the terrestrial model integrated the information to create a runoff model, which identified potential sources of nutrients.

Geospatial Multivariate Classification Results

The ETM+ image dataset of the study area captured an exceptionally heterogeneous environment, with high variability in landuse and landcover. This in turn produced high variability in pixel brightness values and a complex environment to classify. Overall, the more classes were produced, the more inaccuracy in pixel to class allocation was noted. Furthermore, attempts to classify the imagery using bands one through five and seven did not yield ideal results, especially in highly variable settings like urban and agricultural settings. Confusion matrix, although important to the validity of the results and accuracy assessment, was not generated since it requires a reference dataset for ground truth assessment. Assessment of the accuracy relied on visual interpretation using high spatial resolution imagery, as well as through maps, and other available platforms as described earlier in this study.

Unsupervised classification set to 16 classes produced poor results, as pixels were not assigned accurately. Based on photo interpretation, it was visually obvious that there was much confusion, mixed pixels, and heterogeneity in land covers, which seemed homogenous when inspecting the imagery. The landscape pattern, the complexity of the classified features, the transition zones, the different land classes, and the distribution of the classes greatly affected the spectral variation within a class and between classes. Variation in agriculture classes were the result of crop type, lot sizes, planting times, and even direction of plowing. Variations in urban areas were the result of the heterogeneity of the features, their sizes, building materials, and shapes. Hillshade effects were noticeable when setting the ISOCLASS module to 16 classes, and affected the overall integrity of the classification. Due to the hillshade effects the ambient light was not distributed equally across the mountainous scene and as a result altered the spectral signature of the vegetation. What is virtually a single land cover class was classified as multiple classes as seen in Figure 21. The classification picked up differences in the bay water, apparently the effect of the Kishon estuary and Mediterranean interface, with increasing effect in the bay itself. Consequently, the technique produced four water classes, creating distinct clusters of what was supposed to be a rather homogenous body of water. The classification pointed to an anomaly in the bay waters. The anomaly is the result of the interaction of the river estuary and the Mediterranean, and the influence of terrestrial inputs on the spectral signature of normal sea water. The localized influence close to the estuary dissipates seawards to normal oligotrophic water, a process which is illustrated through the different water categories as seen in Figure 21.

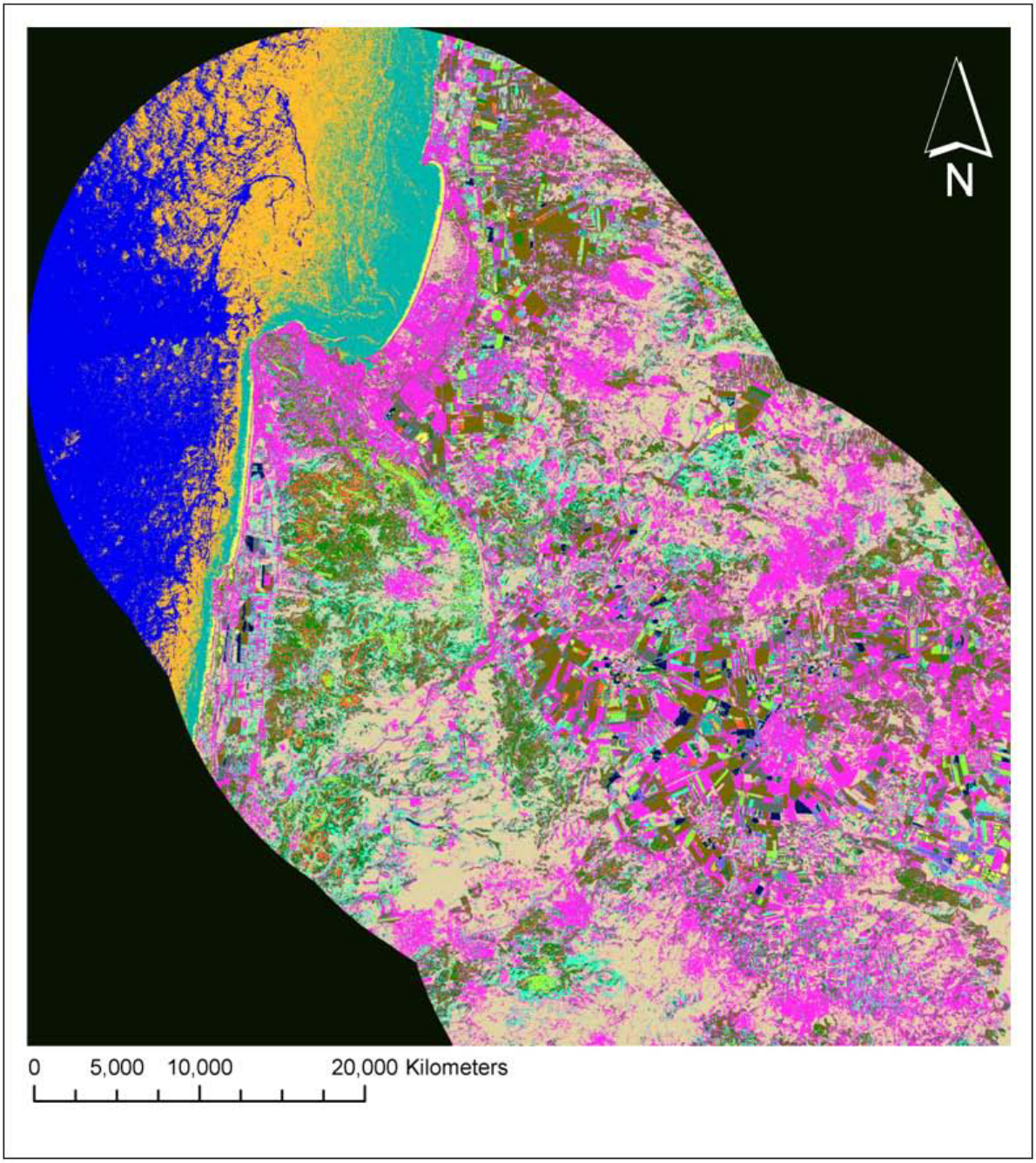

Figure 22: ISOCLASS, 16 Classes, ETM+ May 21, 2000

Source: Sinaya Dayan, 08/01/09

A 13 class image (Figure 22) produced less accurate classification. Confusion in grouping was attributed to the high variation in land cover. The study area includes heterogeneous land covers that occupy a small area and have significant pattern variations. The spatial resolution coupled with the heterogeneity of the landscape affects the spectral variation within a class, increases the number of mixed pixels, and creates a speckling noise. This classification grouped urban/industrial together with bare earth and agriculture areas, as many building materials within the urban scene are taken from the surrounding environment. Although the different land cover types are considerably different physically, they portray a similar spectral signature, which makes discrimination between classes hard to accomplish. Consequently, the ISOCLASS classification of the dataset was not successful in differentiating land features that are notably different to the observer, such as plowed fields and residential areas. The classification, again, grouped the bay water into separate classes, indicating that the bay is influenced by the Kishon estuary, which is the immediate source introduction method of terrestrial inputs. Although, the cluster differentiates the bay waters from deep sea oligotrophic waters, the number of groups is lower than in the 16 class image due to the reduction in the number of classes the clustering produced.

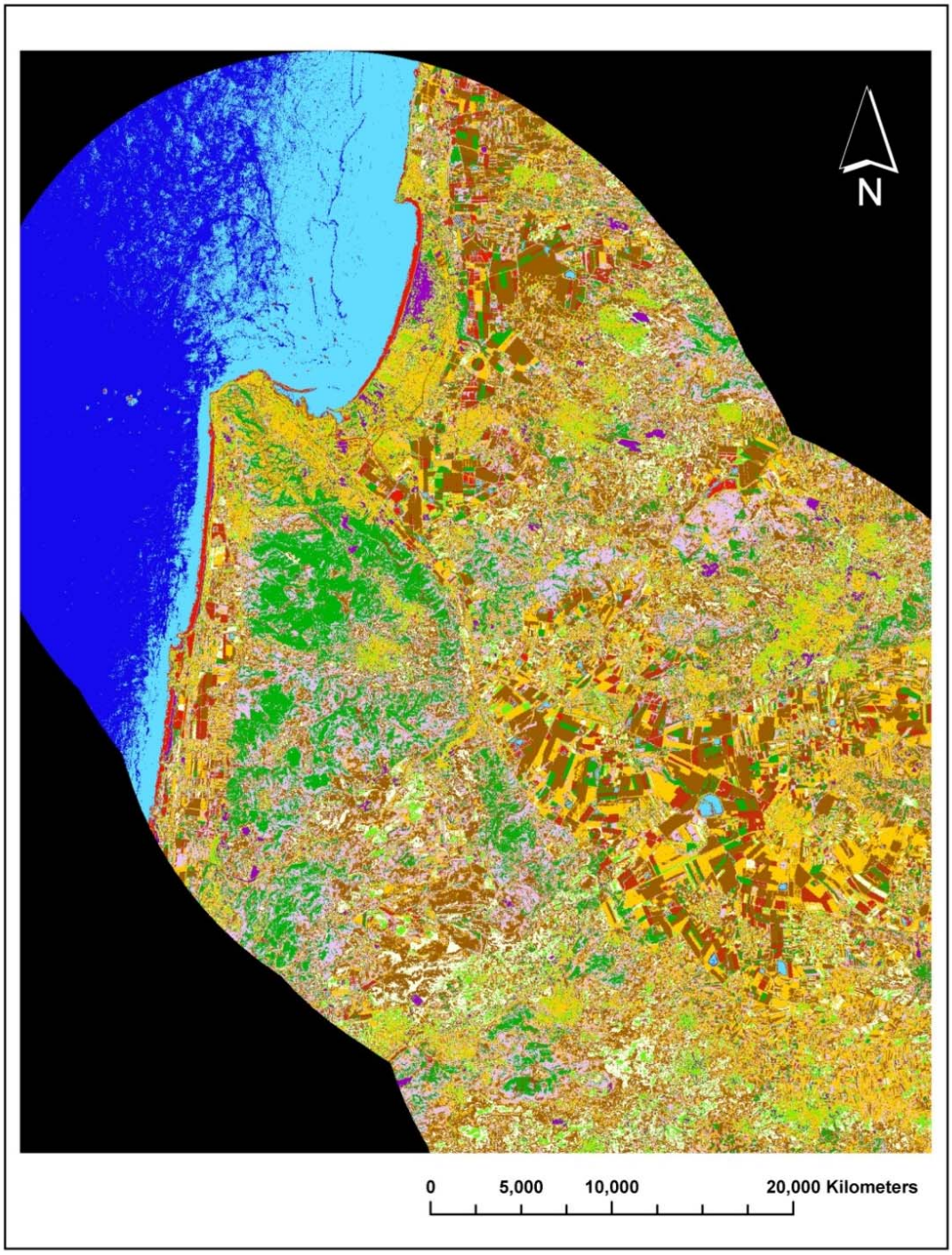

Figure 23: ISOCLASS, 13 Classes, ETM+ May 21, 2000

Source: Sinaya Dayan, 08/01/09

The ISOCLASS method was set to a lower number of classes to correct for the speckling noise. Ultimately, the lesser number of classes the cluster produced, the more confusion of classes was noticed. The reduced number of classes was intended to homogenize the data by assigning stand alone pixels into distinct classes with similar statistical means. Surprisingly, the lower number of classes did not yield homogenized groups, but rather, over-differentiated certain land features, and enhanced heterogeneity and spackling patterns rather than forming more uniform classes. In the 10 class image, seen in Figure 23, the cluster homogenized most vegetation, grouping together evergreen with agriculture crop regardless of the type. It, however, failed to distinguish between urban and bare earth and created a number of separate classes rather than a single class for each land feature. The confusion between urban/industrial areas and bare earth is thought to be the result of similar spectral signatures, caused by the use of natural materials in building blocks in the urban scene. Although the landscape type, shape, and complexity of both land covers vary greatly, they are statistically impossible to differentiate because of the spectral similarities. Also, the complex mountainous terrain along with the typical, light colored, soil in the region i.e., limestone, dolomite, marl, and chalk, show much similarity to the complex urban setting. Consequently, the spatial and spectral resolution of the multispectral imagery, and the use of one through five and seven ETM+ spectral bands were not ideal in producing a suitable classification from which a model can be formed.

PCA provided an alternative data input that replaced the spectral bands used in the prior examples. Using principal components one through six, i.e., PCA1, PCA2, PCA3, etc, included the majority of the information within the image dataset, and allowed a maximized data compression. Essentially, when processing multivariate data, PCA provided a superior technique, as it maximized the variance in one axis while minimizing it on the other axis, a process which

eliminated repetition and enabled a more accurate grouping of the compressed data. Once six principal components were produced, they were classified using the ISOCLASS module, while subjecting the data to identical settings as when using the original spectral bands. 16, 13, and 10 class images were generated (Figures 24, 25, 26). Unlike classifying the original spectral bands, classifying PCA's using ISOCLASS provided better results with decreasing number of classes. Confusion, speckling, mixed pixels and heterogeneity in the 16 and 13 class PC images (Figures 24, 25), were far more dominant. This heterogeneity, along with limited ground control information, affected the ability of the analyst to accurately resolve groupings, and did not allow the integration of the classified image into the runoff model.

Nevertheless, when setting the number of classes to 10, PCA/ISOCLASS technique proved to be extremely useful in resolving the heterogeneity and high variability of the image dataset. The method produced a more suitable classified image (Figure 26) with little confusion, and less mixed pixels. It achieved uniformity within the classes and overall had a more accurate grouping of data relative to the original image (Figure 27). The classified image contains inaccurate classification of plowed field grouped with urban settings, or splitting of the Mediterranean grove attributed to shadows and hill shade effects.

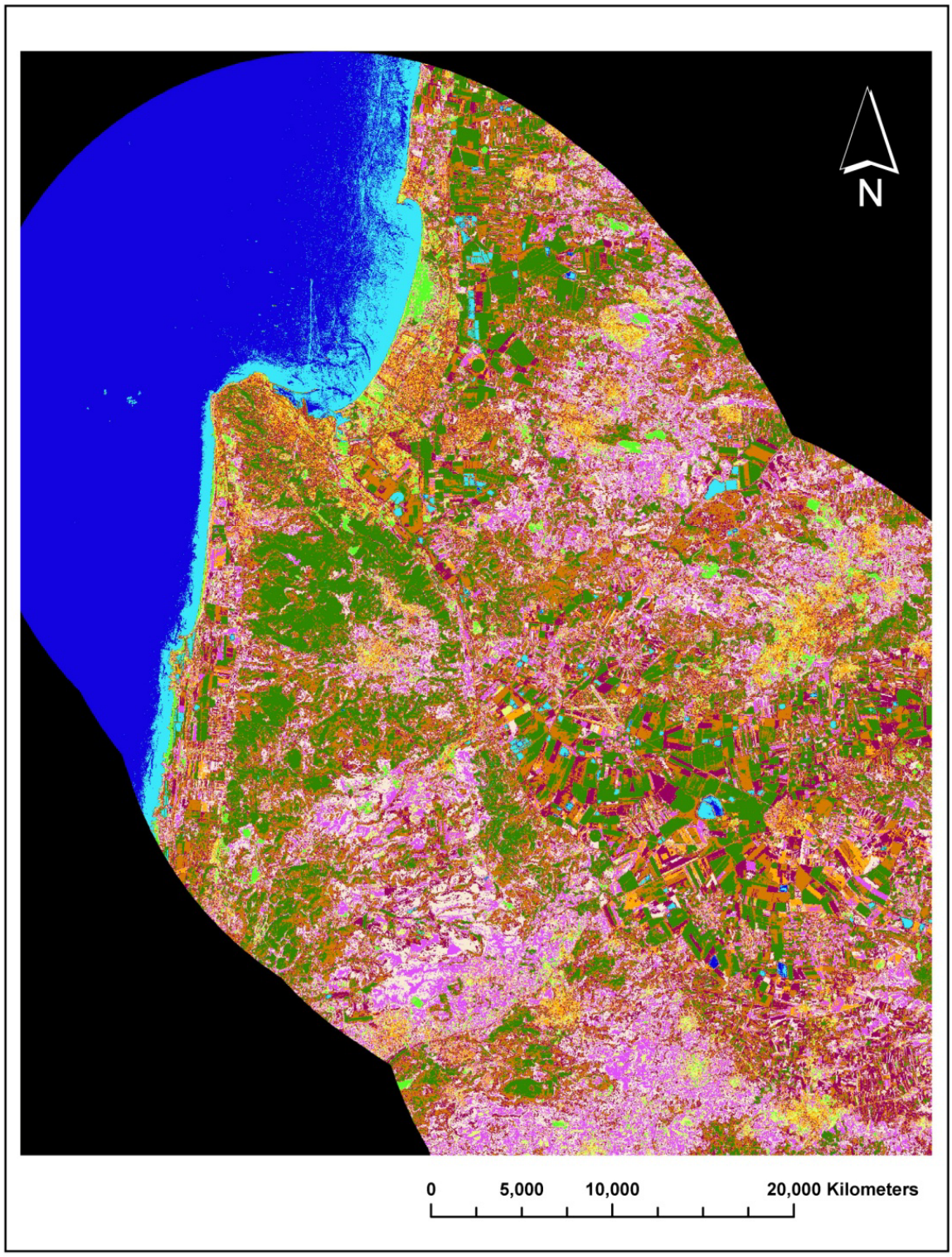

Figure 24: ISOCLASS, 10 Classes, ETM+ May 21, 2000

Source: Sinaya Dayan, 08/01/09

Figure 25: ISOCLASS, Principle Component, 16 classes ETM+ May 21, 2000.

Source: Sinaya Dayan, 08/01/09

Figure 26: ISOCLASS, Principle Component, 13 classes, ETM+ May 21, 2000

Source: Sinaya Dayan, 08/01/09

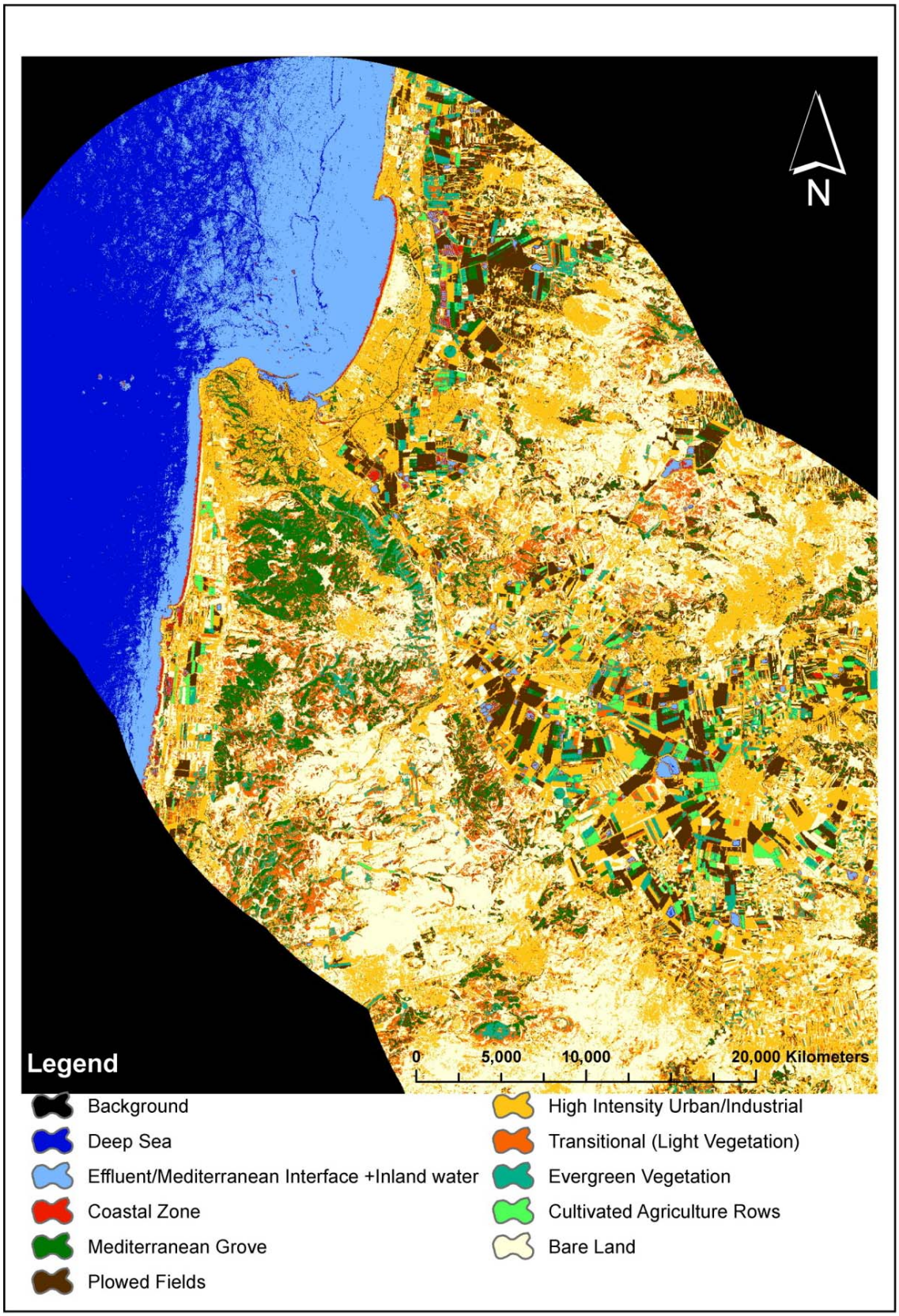

Figure 27: ISOCLASS, Principle Component, 10 Classes, ETM+ May 21, 2000

Source: Sinaya Dayan, 08/01/09

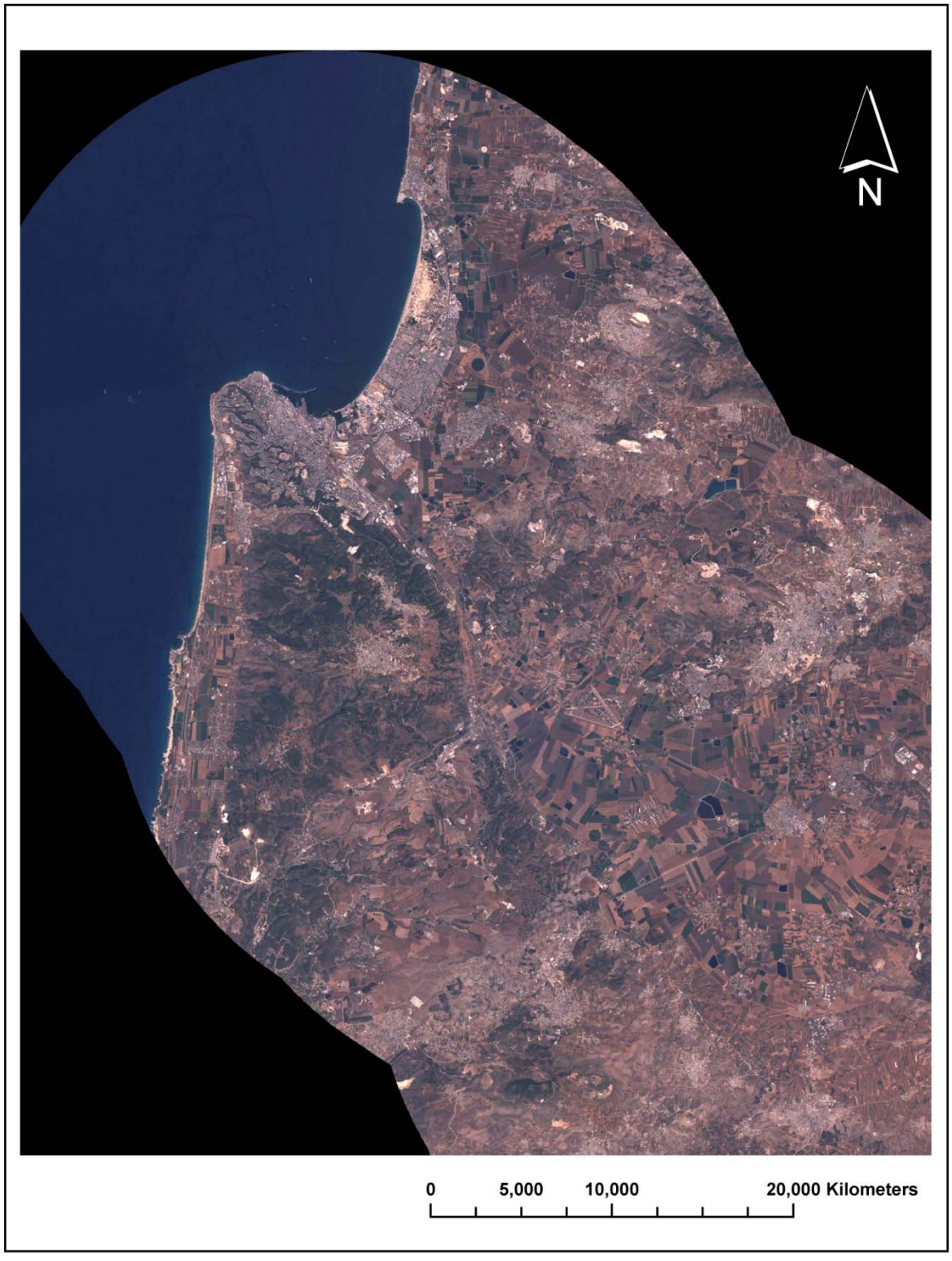

Figure 28: Cropped Image of Haifa Bay, Israel. RGB, ETM+ May 21, 2000

Source: Sinaya Dayan, 08/01/09

Geospatial Runoff Model

A geospatial runoff model was constructed to determine land classes, proposed by this researcher, most likely to introduce higher levels of nutrients into the bay. C factors or runoff coefficients were added to each class as a measure of potential flow. Higher values reflect increased runoff and increased rate of nutrient introduction, considered to be nonpoint source pollution which infiltrates the receiving medium. Examination of the C values revealed that agriculture activities, bare earth, and urban/industrial setting would be considered more likely to contribute to elevated levels of nutrients in the Bay than classes like Mediterranean grove, or evergreen vegetation. Applying thresholds on the runoff coefficient values identified suitable locations for increased levels of nutrients.

Potential land classes, exhibiting favorable conditions for increased runoff and increased levels of nutrients, held a runoff coefficient greater or equal to 0.40. This value included agriculture activities, urban and industrial regions, bare earth and light vegetation areas. The geobiophysical terrestrial model isolated regions featuring such conditions by applying a spatial condition using Map Algebra in ArcMap 9.3. The spatial condition, referred to as **Con** function in ArcMap 9.3, controls the output value for each cell based on whether the cell value meets the specified conditional statement. For instance, in the condition statement **Con** (C_Factor >= 0.40, 1, 0), used in this research, C_Factor represented the file name, 0.40 served as the condition to be tested, while the Boolean values 1, 0 were assigned to true and false outputs respectively. The condition tested the raster image file, identified as C_Factor, by evaluating whether each of the cells had a value higher or equal to 0.40. Cells that met the statement were assigned the Boolean value 1, and cells that had either lower or higher values than the specified value, 0.40, were assigned the Boolean value 0 indicating that condition was not met. The output Boolean values,

1 or 0, created a Boolean raster image, which displayed a single attribute, isolated regions of interest, and enabled the extraction of values that met the condition statement as presented in Figure 28.

The output model encompassed a large area, with varying environmental impact. The relative nutrient contribution is most likely to have an increasing rate of introduction with decreasing distance from the bay. In order to better evaluate sources from which nutrients are introduced to the bay, six spatial buffers were superimposed over the runoff model (Figure 29).

Each of the buffers contained probable source with increasing impact the closer they are to the bay. The 5 km buffer contained regions known to host a vast petrochemical industrial activity, water treatment plants, high intensity metropolitan areas, agriculture land, and marine agriculture (fish ponds). The farther away from the bay towards inland (7 km, and 10 km) the lesser the rate of nutrient introduction is likely to be. A similar concept was applied on the river, which is responsible for transporting terrestrial inputs into the bay. Three buffers 2 km, 5 km, and 7 km were superimposed over the runoff model and contained regions most likely to have highest rate of introduction (Figure 29).

Figure 29: Runoff Model Illustrating Potential Sources.

Source: Sinaya Dayan, 08/01/09

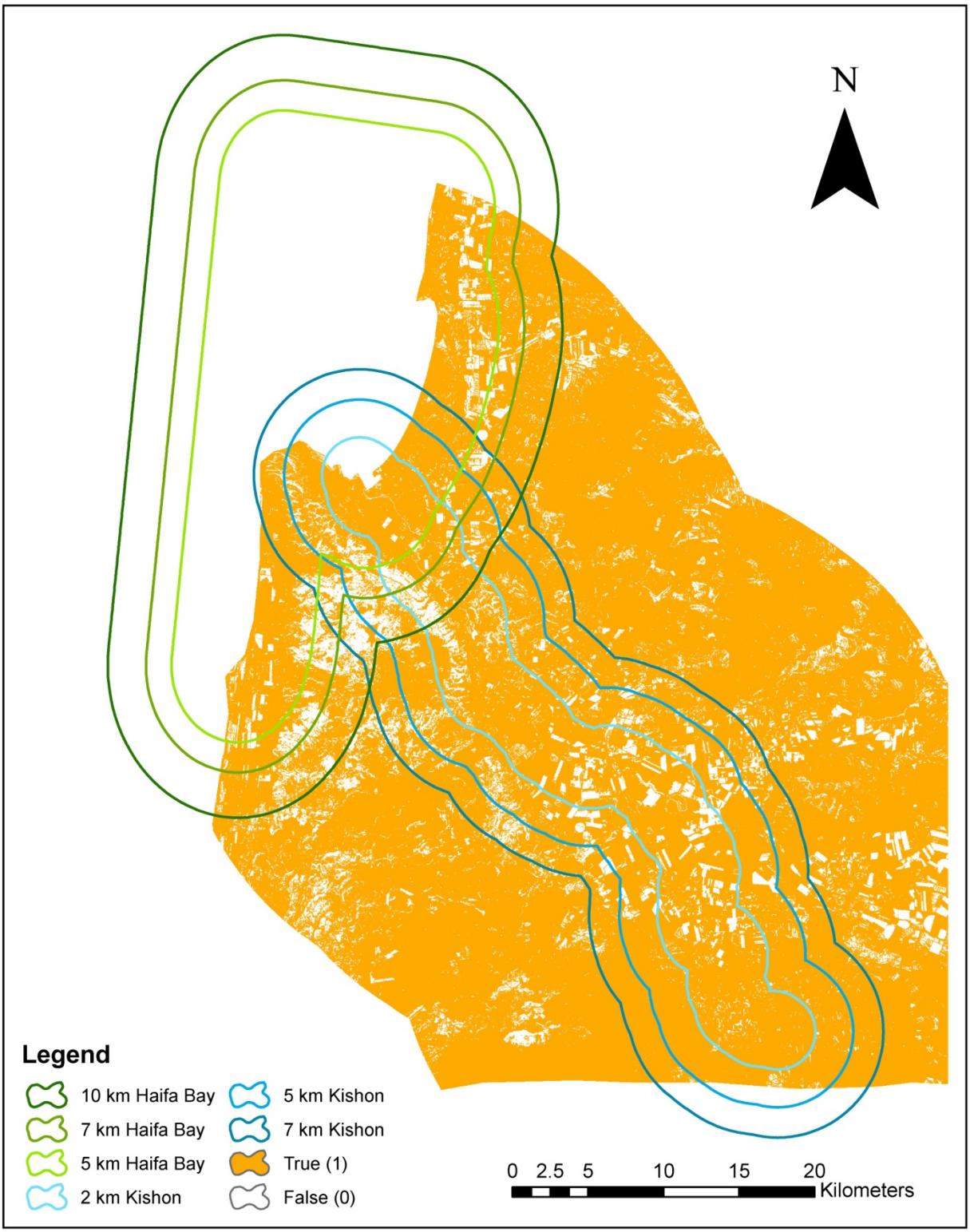

Figure 29: Buffer Analysis Superimposed Over the Runoff Model

Source: Sinaya Dayan, 08/01/09

Marine Geobiophysical Model

The combined action of scattering and absorption progressively diminish the amount of light that propagated through the water column. The degree of attenuation is wavelength dependent and is determined by water clarity/ turbidity (Purkis, 2004). Attenuation in 350-550 nm range is low and is governed by water constituents, which increase the absorption of short wavelengths bands in the visible spectrum. Attenuation in wavelengths greater than 600 nm is rapid, dominated by the absorption characteristics of pure water and is, therefore, not affected by the presence of constituents. The existence of water constituents, such as colored dissolved organic matter, inorganic particles, and chlorophyll affect the absorption/reflection spectra of pure water in the 350-600 nm range, a feature that allows the spectral discrimination of such constituents. Their unique spectral signature is used to highlight the presence of such elements in the water, map their distribution, and quantify their concentration.

The objective of the marine geobiophysical model was to remotely assess the presence and concentration of chlorophyll in the bay waters of Haifa, Israel. Chlorophyll, which is the primary photosynthetic pigment in phytoplankton, absorbs more of the blue and red portion of the electromagnetic radiation than the green portion. The pigment exhibits maximum absorption in the blue region near the 440 nm and maximum reflection in the green range near 550-570 nm. As chlorophyll concentrations increase, the color of the ocean shifts from deep blue to green, making it not only detectable but also measurable by satellite sensors and remote sensing techniques. The assessment was achieved through the use of algorithms sensitive to the absorption/ reflection response of the chlorophyll in the blue and green regions of the spectra, which discriminate chlorophyll from pure water and other constituents. The outcomes of the algorithms were compared with field measurements, reference data, in order to evaluate whether

algorithm results correlate to actual measurement. *In Situ* measurements validated the accuracy of the algorithms, and provided truth data necessary for the assessment and calibration.

Chlorophyll Algorithms for ETM+ Data.

Regression of measured chlorophyll concentrations against the algorithms resulted in a statistical model that made calibration and prediction possible. The ratios utilized spectral properties of chlorophyll, and therefore, provided the required level of discrimination between chlorophyll and other water constituents. The acceptable tolerance of correlation set by this researcher is $R^2 > 0.7$. Any values below 0.7 were considered insufficient correlation coefficients and were, therefore, of no indication of chlorophyll presence in the bay waters.

In the case of this research, small sampling theory, i.e. $n \leq 30$, was tested due to the limited availability of samples of chlorophyll concentrations. Overall, the fewer the sampling intervals, or observations, the larger the variance and the less accurate the correlation becomes. The number of observations in this study was n=19, which was further divided into two groups of: n=8 and n=11 for the two different sampling dates this study examined. The small number of samples contributed to high variance within the data and was not ideal for the analysis performed in this study. Regardless, the small sampling theory approach provided an alternative statistical prediction model with which correlations of image band ratios to chlorophyll concentrations were tested to reveal trends.

The most widely used ratio TM1/TM2 (Blue/Green) was tested, as it utilizes the relative reflectance of blue and green. The ratio takes into account maximum absorbance of chlorophyll in the blue region and minimum absorbance by phytoplankton in the green. The ratio results were regressed against *in situ* measurements and yielded the following results (Figures 30, 31):

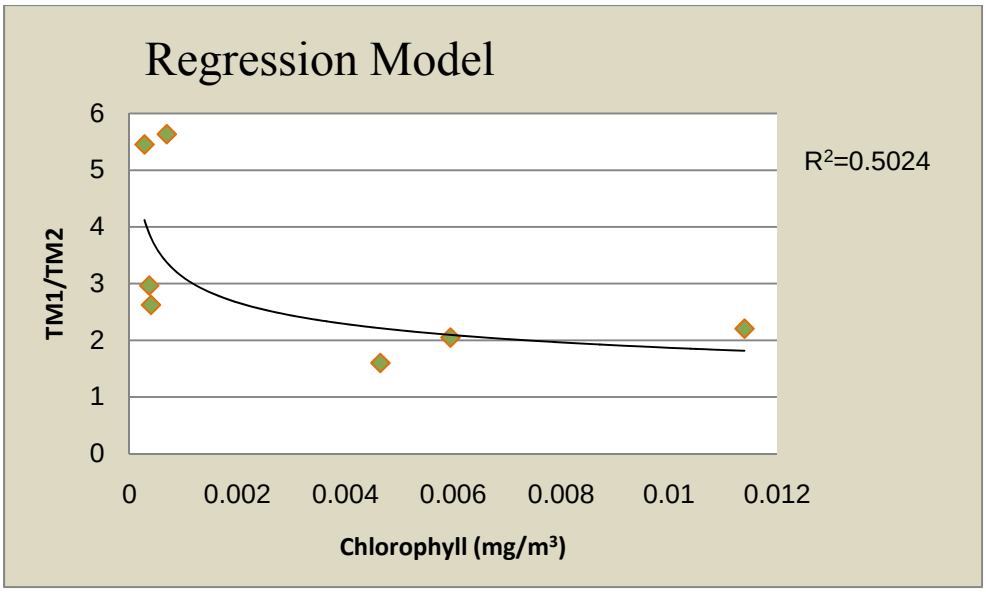

Figure 30: Regression Analysis TM1/TM2 vs. Chlorophyll Concentrations

Source: Sinaya Dayan, 08/01/09

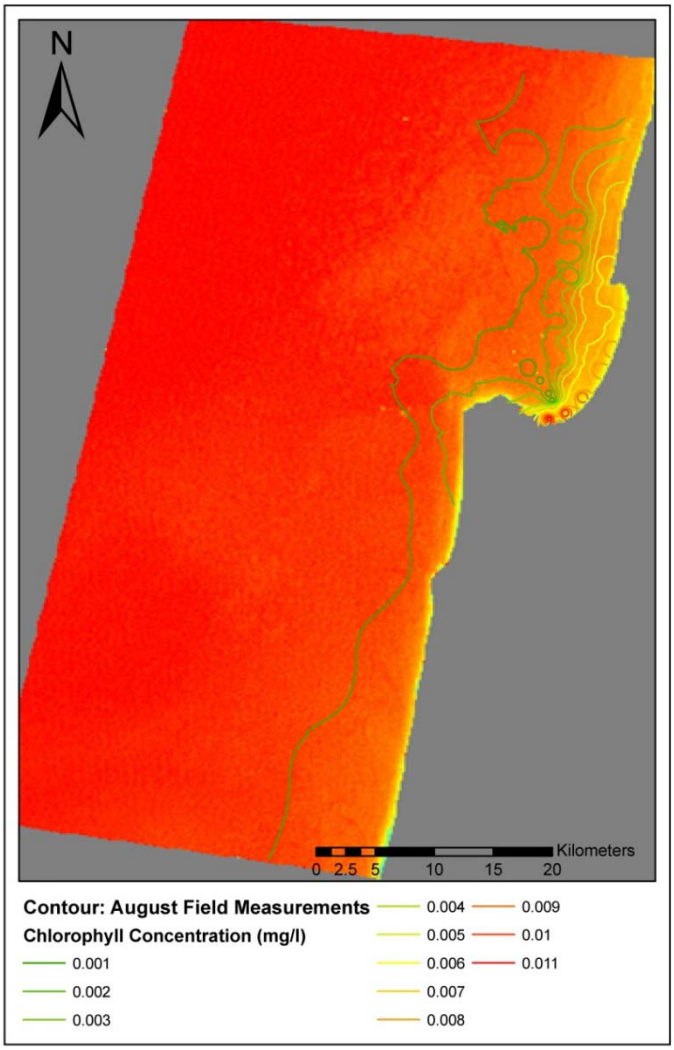

Figure 31: Band Ratio TM1/TM2, Haifa Bay and Portions of Mediterranean Sea

Source: Sinaya Dayan , 08/01/09

The statistical regression did not yield sufficient correlation coefficient (R^2=0.5024), and was considered unlikely to be a good indicator of chlorophyll when using TM bands. Although, it is evident that the image band ratio (Figure 31) highlights the presence of a substance in the bay water, it could not be directly linked to chlorophyll because of the poor statistical correlation.

The algorithm TM3/TM1 (Figures 32, 33) utilizes maximum absorbance by phytoplankton in the blue region and a peak magnitude near the 690 nm caused by chlorophyll fluorescence. Gitelson (1996) found that in Haifa Bay, the measured reflectance values in TM1 and TM3 are inversely correlated. Radiance in the red region (TM3) increases with increase in chlorophyll concentration, while radiance in the blue region (TM1) decreases with increase in chlorophyll concentration. Increase in the radiance of TM3 is attributed to increase in peak magnitude near 690 nm, and the decrease in TM3 radiance is caused by the increase of phytoplankton absorption.

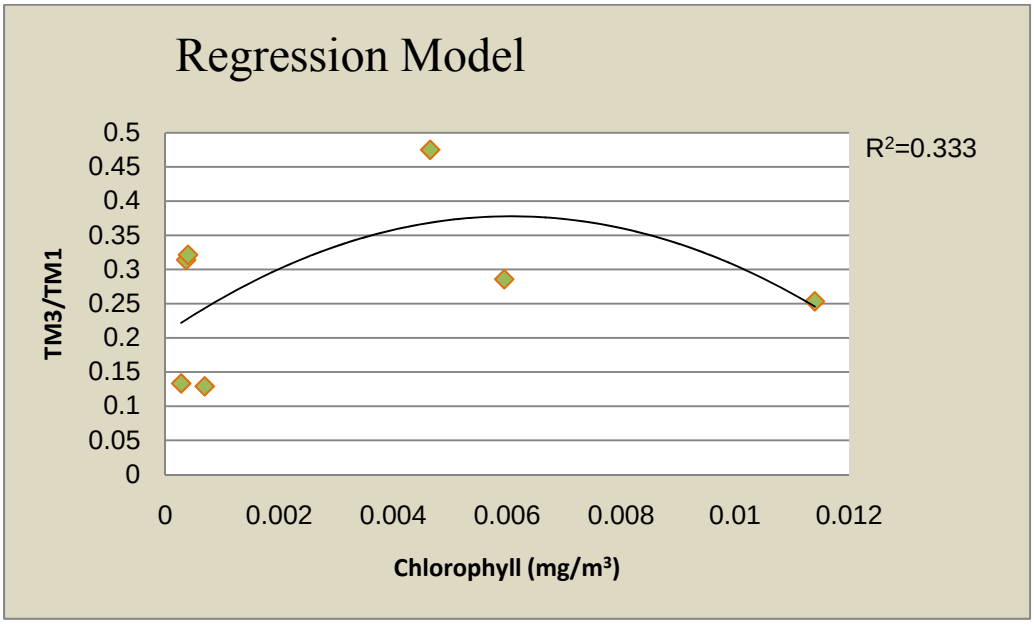

Figure 32: Regression Analysis TM3/TM1 vs. Chlorophyll Concentrations

Source: Sinaya Dayan, 08/01/09

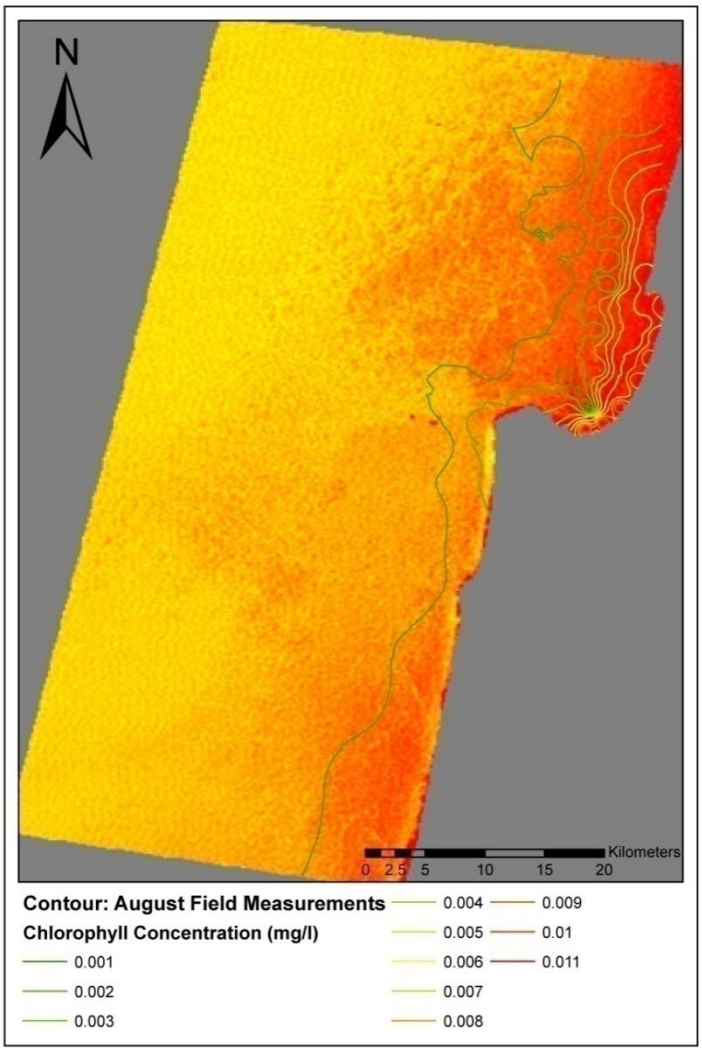

Figure 33: Band Ratio TM3/TM1, Haifa Bay and Portions of Mediterranean Sea

Source: Sinaya Dayan, 08/01/09

The statistical regression (Figure 32) resulted in relatively low correlation coefficient (R^2=0.333), which is thought to be the result of the low chlorophyll concentration measured in the bay during the studied time period. This algorithm was found suitable only in cases where chlorophyll concentration > 3 mg/m^3. Low chlorophyll concentrations diminish the peak reflectance near 690 nm and, therefore, alter the algorithm outcome. As in the prior algorithm, the image ratio algorithm (Figure 33) revealed that around the coastal zone, and more drastically in the bay, chlorophyll or other water constituents were present. The presence of either

chlorophyll and/or water constituents alters the scattering, absorption and attenuation of pure water by their unique spectral behavior i.e., absorption/reflection. While absorption of pure water, for example, is minimal in shorter wavelengths, the presence of chlorophyll increases the absorption in this region, especially in the blue, and causes a shift in the absorption curve. This provides spectral differentiation between chlorophyll and water, allows the discrimination of one from another, and enables the extraction of chlorophyll information from surface water. The presence of chlorophyll is supported by the higher intensity of the red color representing the chlorophyll and possibly other water constituents in the bay. The high intensity of the red color decreases towards deep sea, which consists of pure sea water free of substances, and is therefore linked with the presence of water constituents that alter the spectral response of pure water. The image in Figure 33 contributes to the assumption that the bay does not consist of pure sea water and highlights the presence of water constituents that play an important absorption/reflection role as described earlier.

Lastly, the ratio (TM2-TM3)/TM1 was tested as was found suitable for the detection of low chlorophyll concentration < 3mg/m^3, as it achieved correlation coefficient of R^2=0.8255 (Figure 34). The ratio, again, incorporates the absorption and scattering characteristics of chlorophyll in the blue and green regions. Unlike traditional ratios that use the blue and the green regions, this ratio accounts for the effects of suspended matter on the red region. Mayo et al (1995) determined that reflectance in the region 620-690 nm is primarily dependent on the concentration of suspended matter, which contributes to the scattering effect when present. Radiance in TM3 spectral channel, 630-690 nm, can therefore be subtracted from radiance in TM2 to correct for additional radiance caused by scattering of suspended matter.

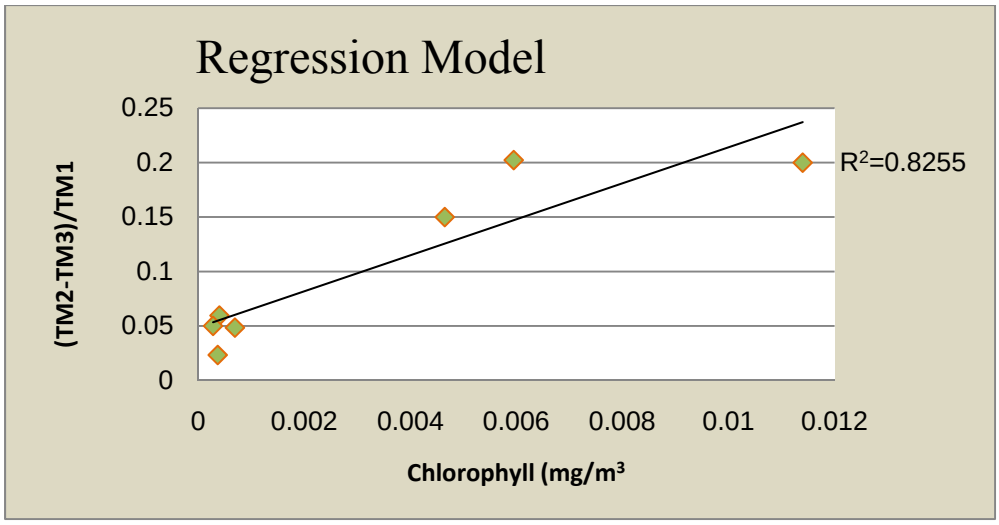

Figure 34: Regression Analysis (TM2-TM3)/TM1 vs. Chlorophyll Concentrations

Source: Sinaya Dayan, 08/01/09

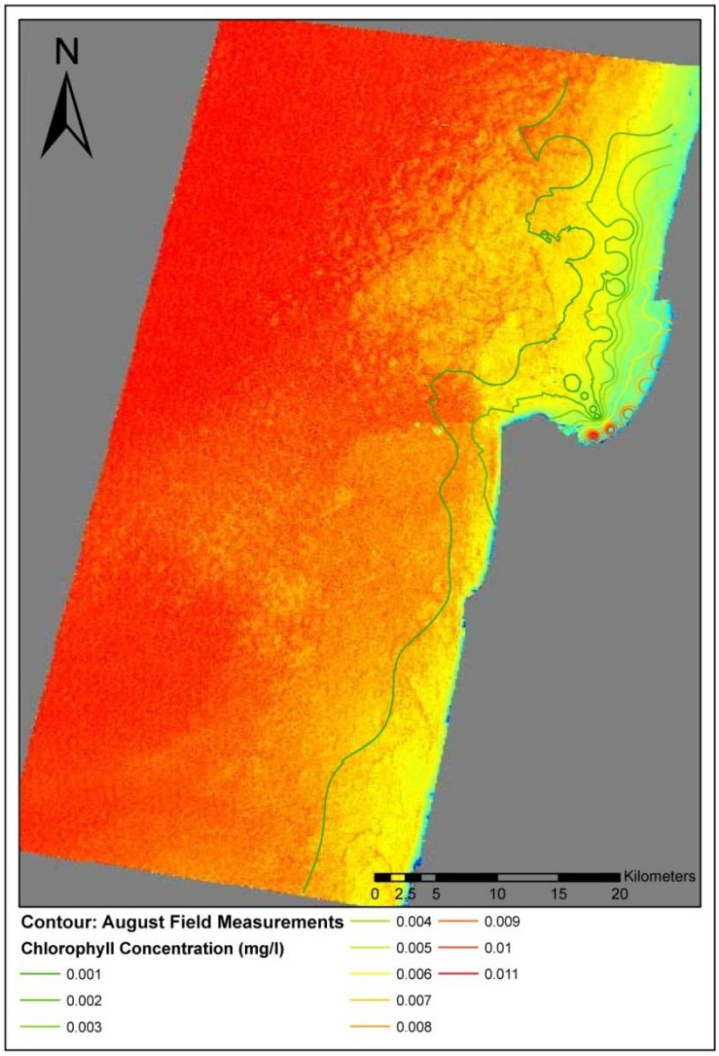

Figure 35: Band Ratio (TM2-TM3)/TM1, Haifa Bay and Portions of Mediterranean Sea

Source: Sinaya Dayan, 08/01/09

Both the image band ratios (Figure 35), as well as, the statistical regression provide sufficient support that this algorithm successfully isolates and highlights chlorophyll. Not only that high correlation between field reference measuremetns of chlorophyll and the algorithm output was found, but support is also provided through visual inspection of the raster image of the algorithm. The presence of chlorophyll,symbolized in yellow, is apperant throughout the Israeli coast. Its concentration, however, is intensified in the bay and the northern shore, as symbolized in green, and is different from oligotrophic water, symbolized in red. This algorithm was found satisfactory for the highly varied waters of Haifa Bay as it demonstraed high correlation to field measurments.

The examination of the relationship between *in situ* measured chlorophyll concentrations and reflectance values included several models: linear, polynomial, exponential, and power transformations. Although all raster algorithms highlited the presence of water constituents, only the linear model (TM2-TM3)/TM1) correlated well with the field measurements and was considered an accurate assessment method.

Chlorophyll Algorithms for MERIS Data.

The relationship between chlorophyll concentrations and several ocean color algorithms were tested on MERIS data. Although the spatial resolution of the MERIS sensor is not ideal for this regional analysis, its spectral resolution is most suitable for ocean color analysis, and is likely to reflect conditions with high accuracy.

In situ measurements from March 22-24, 2004 were plotted against several algorithms to establish a relationship between the spectral bands and chlorophyll concentrations measured in the bay water. Since MERIS pixel size is relatively large some pixels contained two or more samples. In cases where more than one sample was contained within a pixel the arithmetic mean

of chlorophyll concentrations of all sampling stations within that pixel was used. Using mean values reduced the number of samples from eight to five.

Morel and Gentili (2009) used band ratio R490/R555 to quantify algal content in oceanic settings. Using MERIS spectral channels, the algorithm R490/R560 regressed against chlorophyll concentrations yielded correlation coefficient of R^2=0.8192 (Figure 36). This algorithm utilizes the blue and green regions, which correspond with maximum absorption and minimum absorption by chlorophyll respectively. The image band ratio captured the biological process taking place in the Southeastern Mediterranean. From the results of the R490/R560 algorithm and based on the high statistical correlation, it is evident that the light green/yellow color (Figure 37) near coastal regions represents productive waters. The trend clearly indicates that the coastal stretch could be classified as eutrophic.

Gitelson et al (1996), Gitelson et al (2000), and Iluz et al (2003), all utilized R440/R550 and R520/R550 to assess surface chlorophyll in oligotrophic waters. Using similar methods, reflectance ratios R442.5/R560 and R520/R560 (MERIS corresponding spectral channels) were regressed against chlorophyll measurements and yielded the following results: (Figures 38, 40)

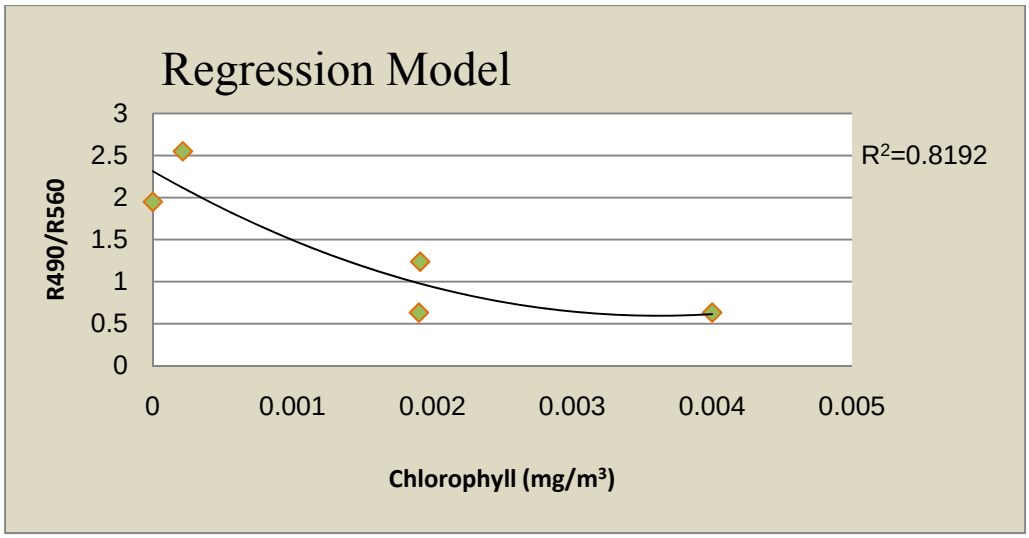

Figure 36: Regression Analysis R490/R560 vs. Chlorophyll Concentrations

Source: Sinaya Dayan, 08/01/09

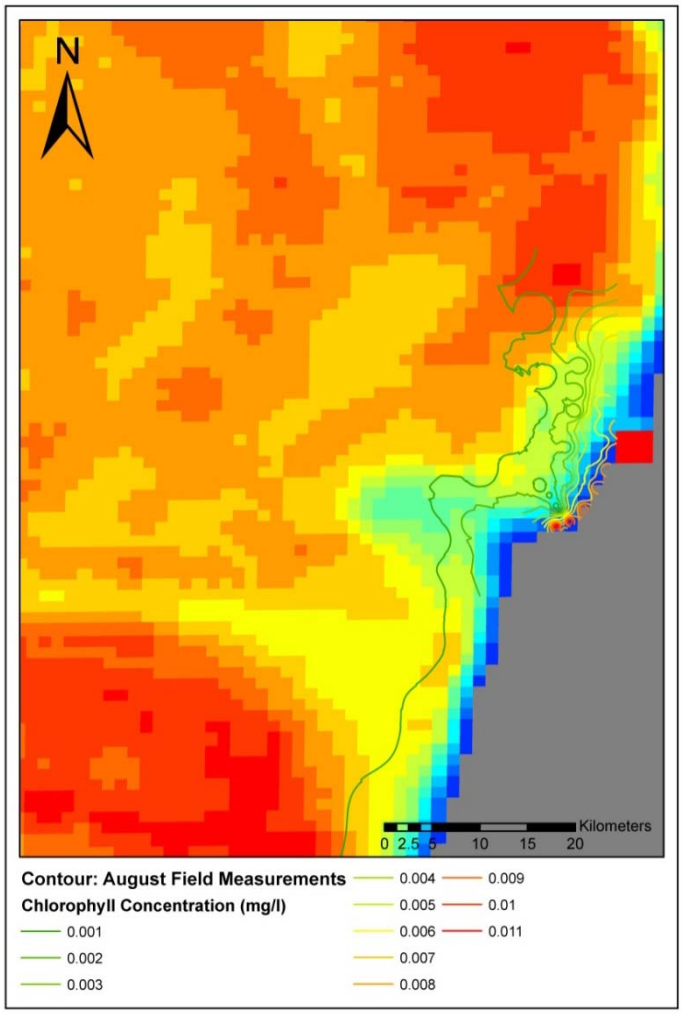

Figure 37: Band Ratio R490/R560, Haifa Bay and Portions of Mediterranean Sea

Source: Sinaya Dayan , 08/01/09

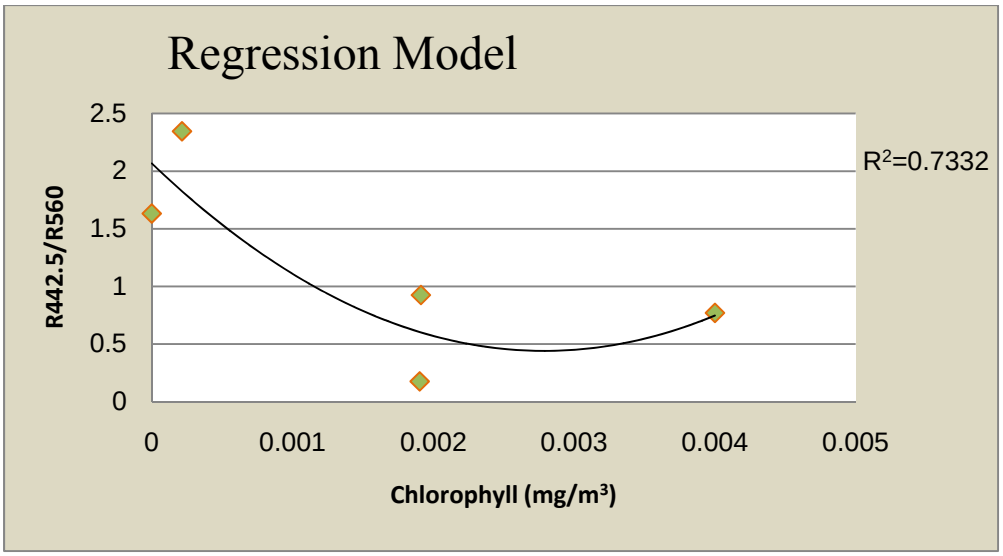

Figure 38: Regression Analysis R442.5/R560 vs. Chlorophyll Concentrations

Source: Sinaya Dayan , 08/01/09

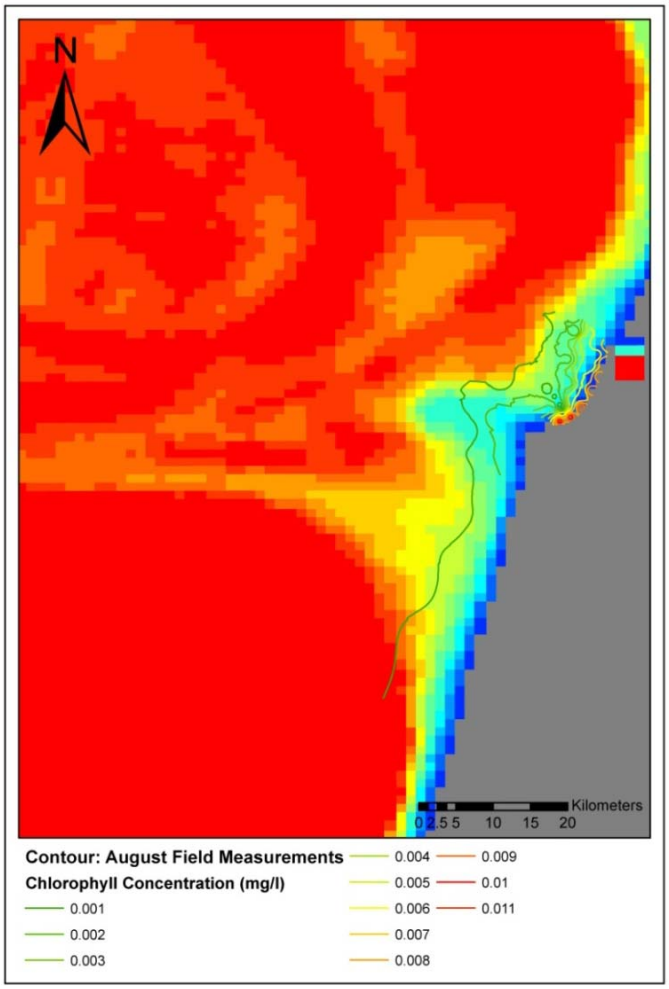

Figure 39: Band Ratio R442.5/R560, Haifa Bay and Portions of Mediterranean Sea

Source: Sinaya Dayan, 08/01/09

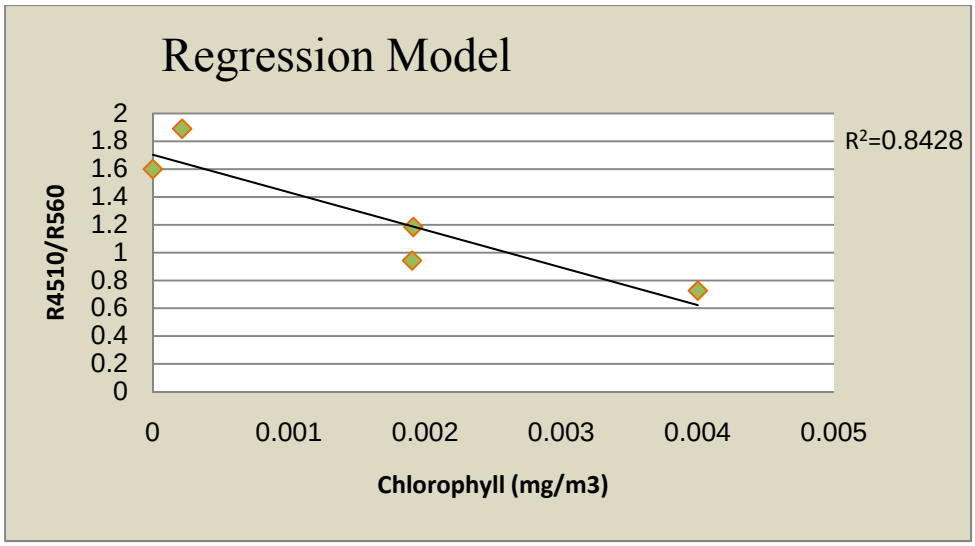

Figure 40: Regression Analysis R510/R560 vs. Chlorophyll Concentrations

Source: Sinaya Dayan, 08/01/09

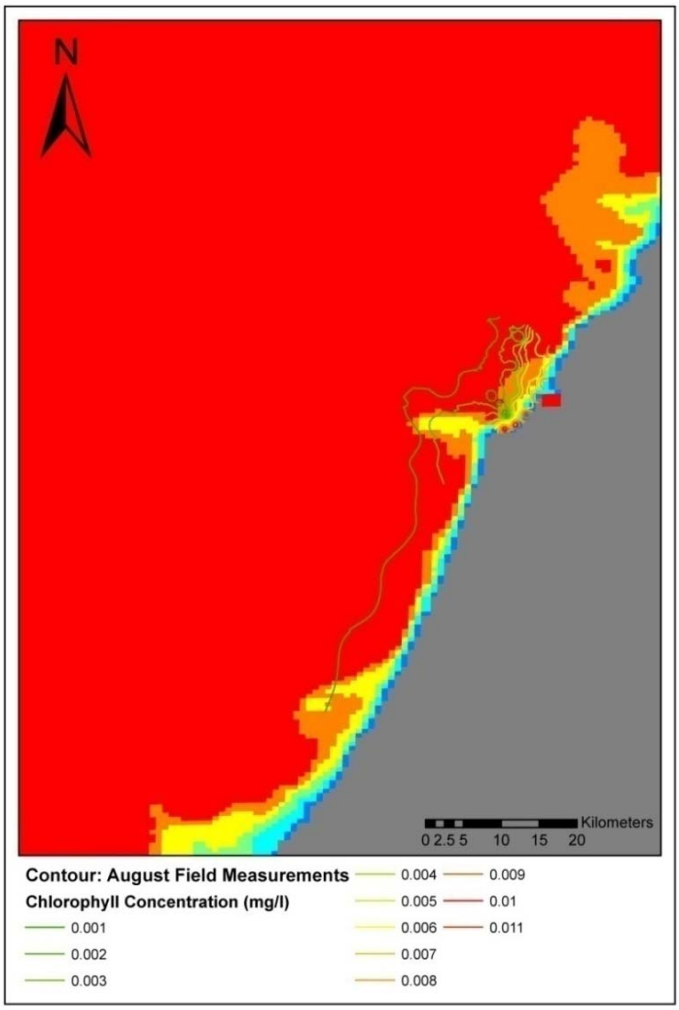

Figure 41: Band Ratio R510/R560, Haifa Bay and Portions of Mediterranean Sea

Source: Sinaya Dayan, 08/01/09

The regression models of both algorithms, R442.5/R560 and R510/R560 (Figures 38, 40 respectively) show sufficient correlation to chlorophyll measurements, and demonstrate that those algorithms are extremely effective in oligotrophic water as the Mediterranean. In previous research, the algorithm R443/R550 enabled the prediction of chlorophyll concentration with 0.08 mg/m^3 and 0.013 mg/m^3 estimation errors (Gitelson, 1996; Iluz et al, 2003). The algorithm is most suitable in areas where suspended terrestrial inputs are minimal, as terrestrial inputs may mask the spectral signature of chlorophyll and alter the outcome of the algorithm. The algorithm R520/R560 (R510/R560 MERIS channels) is interchangeable with the ratio R443/R550, as they both employ a ratio reflectance within the blue and green regions. The band ratio image (Figure 41) achieved uniformity in non coastal areas as would be expected in oligotrophic deep waters, whereas in coastal areas and the research area it emphasized the presence of chlorophyll. The high statistical correlation between the measured concentration of chlorophyll and the reflectance ratio supports this assumption and validates the ability of the algorithm to remotely model and extract chlorophyll information from marine systems.

Of all algorithms that were tested, R520/R560 achieved highest correlation between measured and reflectance values (R^2=0.8428), and was, therefore, used to predict chlorophyll concentration using the following function:

(Eq. 5) Chlorophyll-a (mg/m^3) = $0.914\ (R440/R550)^{-1.86}$

Where 0.914 represents the absorption coefficient (a) and -1.86 represents the scattering coefficient (b). The reflectance channel R440 was replaced with R510, as it provided best fit to the measured values in this study.

In order to validate the statistical model, chlorophyll prediction results were regressed against actual chlorophyll concentrations and achieved R^2=0.9272 (Figure 42) with 0.172855

mg/m^{3}error of estimation. The high correlation between predicted chlorophyll concentrations and actual concentrations of chlorophyll confirmed that the model has the ability to adequately predict chlorophyll concentrations for the inspected body of water.

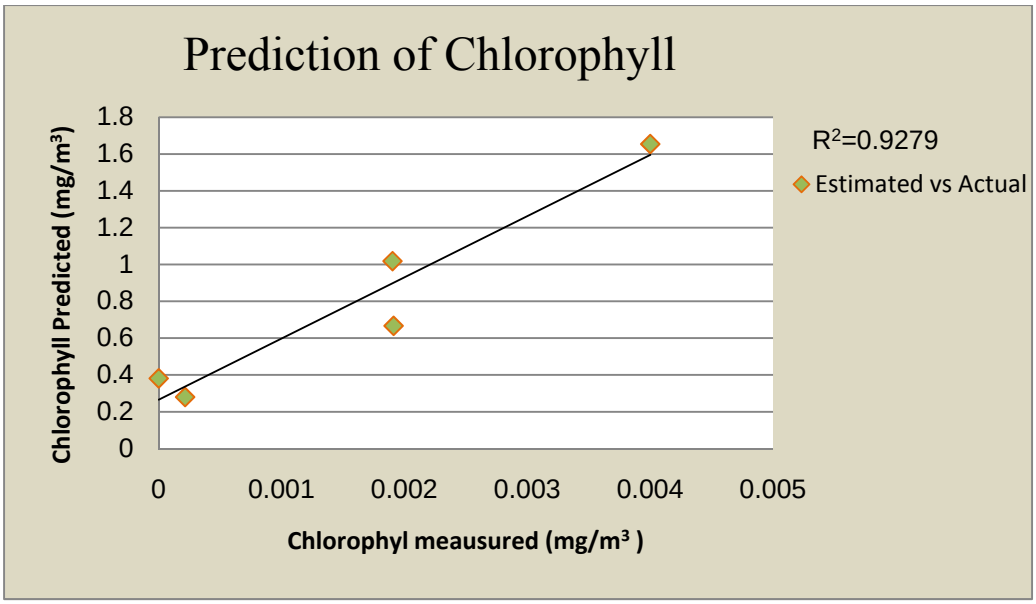

Figure 42: Estimated Chlorophyll Concentrations vs. Actual Chlorophyll Concentrations

Source: Sinaya Dayan, 08/01/09

CHAPTER IV

Conclusions and Future Research

Conclusions

The *terrestrial geobiophysical model* successfully illustrated potential sources for nutrient runoff using multivariate data. The runoff model validates the assumption that diffuse or non point source pollutants originate inland; particularly in urban, industrial, and agriculture environments. The research demonstrated the importance and ability of remote sensing and geobiophysical modeling in solving environmental issues, and in adding value to existing assessment techniques.

In the classification results, the 10 class principle component isoclass image provided best results, as it accounted for maximum variability in the data, captured the internal structure of the data, and resolved the high variability the dataset presented. The extracted information, displayed in the classified image (Figure 26), was considered suitable to be integrated into the runoff model, as it demonstrated sufficient class differentiation and isolation necessary to determine the sources of nutrient transported to sea.

The intersections between the bay buffers and the river buffers isolated regions with harsh environmental impacts on the quality of the bay waters adversely affecting the marine setting. The severity of the potential impact and relative contribution is inversely correlated to the distance from Haifa Bay and the Kishon River; the larger the distance is, the smaller the impact on the marine environment is likely to be. Depending on the allocation of resources and severity of the environmental impact, perhaps it would be best to focus attention and resources on areas with higher relative contribution captured by the intersections of the buffers.

Although the majority of potential sources in the Haifa Bay region are known, delivering an output geobiophysical model that emphasizes such sources provides a focused spatial reference and facilitates an immediate response time. Moreover, modeling is achieved effectively through the vast availability of satellite imagery and the continuous data collection, and can be done frequently while allowing constant monitoring.

The *marine geobiophysical model* achieved successful results utilizing two sensors that differ in their spectral and spatial characteristics. The use of ocean color algorithms and field measurements facilitated the detection of chlorophyll in the oligotrophic Mediterranean Sea, particularly in Haifa Bay. The research demonstrated an efficient alternative method to the conventional monitoring process, which could be used as a powerful tool for research and for monitoring the marine environment.

Data acquired by two sensors, ETM+ and MERIS, show variation in accuracy and correlation to field measurements, as they differ in their spectral and spatial attributes. MERIS is an ocean color sensor and is more suitable to be used for assessing chlorophyll presence in oceanic systems. Nevertheless, despite the insufficient spectral resolution, ETM+ algorithms were still able to provide adequate results, though, not with as high correlation as MERIS. Both sensors make use of the visible spectra or more specifically the blue and green regions. Even though R442.5/R560 and R510/R560 are interchangeable algorithms, the last showed higher correlation to *in situ* measurements (R^2=0.8428) of chlorophyll and was considered to be the best prediction model for Haifa Bay. This assumption was validated by comparing actual chlorophyll measurements to the algorithm estimated values. Results showed high correlation between actual and estimated (R^2=0.9272) suggesting that the algorithm could be used for future research.

Statistical regression of the TM1/TM2 algorithm did not yield sufficient correlation coefficient (R^2=0.5024), and was considered unlikely to be a good indicator of chlorophyll when using TM bands. Although, it is evident that the image band ratio (Figure 31) highlights the presence of a substance in the bay water, it could not be directly linked to chlorophyll because of the marginal statistical correlation.

The TM3/TM1 ratio, although highlighted the presence of a substance, this researcher was not able to resolve the nature of it due to a poor statistical correlation to reference field data. Since the research could not provide the desired statistical support between the algorithm result and chlorophyll concentration, the substance could not be directly linked with chlorophyll presence.

The statistical regression (Figure 34) for (TM2-TM3)/TM1 resulted in high correlation coefficient (R^2=0.8255), and was, therefore, considered very useful in remote assessment of chlorophyll. A visual inspection of the image ratio, (TM2-TM3)/TM1, revealed that the southern and the northern coasts show discrepancies in color appearance, which is indicative of the higher chlorophyll concentration found in and near the bay. The similarity between Haifa Bay and the northern shore is most likely the result of longshore currents transporting phytoplankton from the bay, where concentrations are highest, to the north.The algorithm eliminates the possibility that the spectral response is of suspended inorganic particles, since occurence and distribution of suspended sediments, caused by wave action, should be uniform throughout the coastal stretch. The lack of uniformity along with the statistical correlation suggest that the optical variation is the result of the presence of chlorophyll, which is intense in the bay, particularly near the Kishon estuary, and decreases when moving towards deep sea

Although all image band ratio algorithms highlited the presence of water constituents, only the linear model (TM2-TM3)/TM1) correlated well with the field measurements and was considered an accurate assessment method.

MERIS data, although not an ideal spatial reolution required for the scale of this study, was extremely usefull spectrally,as it featured high spectral resolution both in the number of bands as well as the recorded wavelength interval.

From the results of the R490/R560 algorithm and based on the high statistical correlation, it was evident that the light green/yellow color (Figure 37) near coastal regions represented productive waters. The trend clearly indicated that the coastal stretch could be classified as eutrophic and significantly different from the oligotrophic waters towards deep sea. Support for these findings is found in field measurements of chlorophyll concentration, which clearly highlights a trend of decreasing concentrations with increasing distance from the shore. R443/R550 algorithm is very useful for assessing chlorophyll concentrations, as it displays maximal and minimal sensitivity to chlorophyll concentrations and described by most research as the ideal prediction model. Of all algorithms that were tested, R520/R560 achieved highest correlation between measured and reflectance values (R^2=0.8428).

Chlorophyll prediction results were regressed against actual chlorophyll concentrations and achieved R^2=0.9272 (Figure 42) with 0.172855mg/m^3error of estimation. The results confirm that the model has the ability to adequately predict chlorophyll concentrations for the inspected body of water, and would be suitable for monitoring the water quality in Haifa Bay.

The algorithms utilize the spectral properties of chlorophyll, absorption and reflection, and are presumed chlorophyll specific with little interference of other optically active substances. Still, suspended particulates and dissolved organic material mask the spectral response of

chlorophyll and may affect the results. It would have been beneficial if *in situ* measurements of both suspended particulates and suspended organic matter were available to determine their relative influence of the prediction algorithms.

For all statistical regression models the number of observations as well as their distribution was not ideal, as sample sizes were significantly small and represented a linear profile. In the case of this research, a small sampling theory, i.e. $n \leq 30$, was tested due to the limited availability of samples of chlorophyll concentrations. Overall, the fewer the sampling intervals, or observations is the greater the probability that it may lead to inaccurate results, larger variance, and to the less accurate the correlation. As this study made use of available samples and did not conduct additional data collection, it was not possible to set the desired sample size and have an ideal number of observations. This research assumes a lower precision in the model results and acknowledges the need for a larger number of samples for a more reliable set of terrestrial and marine geobiophysical models.

Future Research

Future research of runoff modeling should construct comprehensive models that account for atmospheric depositions as well as the terrestrial inputs from both Non Point Source and Point Source. A complete nutrient budget would be beneficial to determine relative contribution and allow more accurate identification of sources. A more detailed research of watersheds that feed the bay, as well as generating and identifying sub-classes, would allow better analysis and offer a far more extensive approach than what this research examined.

This researcher recommends that future research collect a more adequate sample size, $n>30$, which is both large as well as properly spatially distributed within the study area.

Increasing the number of samples will increase the reliability of the geobiophysical model and accuracy of its results.

Future research could examine the effect of other substances on the optical response of chlorophyll. Although the marine model is assumed transferable to other geographic regions, careful attention must be given to the uncertainties in the model. It is of high importance to assess the results of the algorithm prior to any analysis, as results may vary significantly depending on the body of water. Ground corroboration and collection of *in situ* spectral measurements would add further credibility to any future research, as it would record real time optical response and reduce atmospheric interference.

Regional analysis would benefit from the use of airborne multispectral systems, as they would be time and area specific, have the required spectral and spatial resolutions, and would reduce the atmospheric interference. Airborne systems could facilitate a tailored monitoring approach, which may supplement and enhance the traditional spaceborne monitoring techniques. Both airborne as well as spaceborne systems have the potential to become the primary monitoring method.

CHAPTER V

Bibliography

Aiken, J., Moore, G.F., & Holligan, P.M. (1992) *Remote sensing of oceanic biology in relation to global climate change*. Journal of Phycology, 28(5), 579-590.

Ball, G. H., & D. J. Hall. (1965). *A novel method of data analysis and pattern classification*. Menlo Park, California: Stanford Research Institute.

Brumfield, J.O., Sanderson, D., Farrar, I., Langdon, J.A.., Hugh, H., Bloemer, L., & Oberly, R. (1997). *High resolution digital color infrared image and vegetation associations in cartographic models of Appalachian mountainous wetlands of Canaan Valley.* Retrieved December 1, 2008, from http://www.kfunigraz.ac.at/geowww/hmrsc/pdfs/hmrsc5/BlEA_hm5.pdf

Bukata, R.P., Jerome, J.H., Kondratyev, K.Y., & Pozdnyakov, D.V. (1995). *Optical properties and remote sensing of inland and coastal waters. Boca Raton: CRC Press.*

Canada Center of Remote Sensing. (2008). *Ocean Colour & phytoplankton Concentration.* Retrieved April 20, 2009, from http://www.ccrs.nrcan.gc.ca/resource/tutor/fundam/chapter5/27_e.php

Carpenter, S.R., Caraco, N.F., Correll, D.L., Howarth, R.W., Sharpley, A.N., & Smith, V.H. (1998). *Nonpoint pollution of surface waters with phosphorous and nitrogen.* Ecological applications, 8(3), 559-568.

Central Bureau of Statistics. (2007). *Israel in Figures.* Retrieved March 31, 2009, from http://www1.cbs.gov.il/publications/isr_in_n08e.pdf

Cermeno, P., Dutkiewicz, S., Harris, R.P., Follows, M., Schofield, O., & Falkowski, P.G. (2008). *The role of nutricline depth in regulating the ocean carbon cycle.* PNAS, 105(51), 20344-20349.

Cloern, J.E. (2001). *Our evolving conceptual model of the coastal eutrophication problem.* Marine Ecology Progress Series, 210, 223-253.

European Space Agency. (2009). *Envisat overview.* Retrieved May 05, 2009, from http://www.esa.int/esaEO/SEMWYN2VQUD_index_0_m.html

Fitzpatrick, F.A., Knox, J.C., & Whitman. H.E.(1999). *Effects of historical land-cover changes on flooding and sedimentation, North Fish creek, Wisconsin*. USGS Water-Resources Investigations Report 99-4083. U.S. Department of the Interior, U.S.Geological Survey, Reston, VA.

Giovanardi, F., & Vollenweider, A. (2004). *Trophic conditions of marine coastal waters: experience in applying the Trophic Index TRIX TO two areas of the Adriatic and Tyrrhenian seas.* J. Limnol, 63(2), 199-218.

Gitelson, A. Mayo, M., Yacobi, Y.Z., Karnieli, A., & Kress, N. (1996). *Reflectance spectra of polluted marine waters in Haifa Bay, Southeastern Mediterranean: Features and Applications for remote estimation of chlorophyll concentration.* Isr. J. Earth Sci, 45, 127-136.

Gitelson, A.A., Yacobi, Y.Z., Schalles, J.F., Rundquist, D.C., Han, H., Stark, R., et al. (2000). *Remote estimation of phytoplankton density in productive waters.* Arch. Hydrobiol. Spec. Issues Advanc. Limnol, 55, 121-136.

Grall, J., & Chauvaud. L. (2002). *Marine eutrophication and benthos: The need for new approaches and concepts.* Global Change Biology, 8(9), 813-830.

Gunther, F.J. (1981). *Statistics for landsat data users.* National Aeronautics and Space Administration

Hager, L.S. (ED.). (2008). *Land Development Handbook* (3rd ed.). New York: McGraw-Hill, Inc

Hassan, D. (2005). *Protecting the Marine Environment from Land-Based Sources of Pollution: Towards Effective International Cooperation.* Burlington: Ashgate.

Herut, B., Collier, R., & Krom, M.D. (2002). *The role of dust in supplying nitrogen and phosphorus to the Southeast Mediterranean.* Limnology and Oceanography, 47(3), 870-878.

Herut, B. & Kress, N. (1997). *Particulate metals contamination in the Kishon River estuary, Israel.* Marine Pollution Bulletin, 34(9), 706-711.

Hessen, D.O., Hinder, A., & Holtan, G. (1997). *The significance of nitrogen runoff for eutrophication of fresh water and marine recipients*. Ambio, 26(5), 321-325.

Hill, M.K. (2004). *Understanding environmental pollution*. (2nd ed.). New York: Cambridge University press.

Huertas, I.E., Rios, A.F., Garcia-Lafuente, J., Makaoui, A., Rodrigueze-Galvez, S., Sanchez-Roman, A., et al. (2009). *Anthropogenic and natural CO2 exchange through the straits of Gibraltar.* Biogeosciences Discussions, 6, 647-662.

Hugh, H., Bloemer, L., Brumfield, O.J., Farrar, I., Sanderson, D., Langdon, J.A., & Oberly, R. (1997). *Cartographic representation using a 3D Geographic Information System for the assessment of wetlands in mountainous areas.* Retrieved December 1, 2008, from http://www.kfunigraz.ac.at/geowww/hmrsc/pdfs/hmrsc5/BlEA_hm5.pdf

Iluz, D., Yacobi, Y.Z., & Gitelson, A.A. (2003). *Adaptation of an algorithm for chlorophyll-a estimation by optical data in the oligotrophic Gulf of Eilat*. International Journal of Remote Sensing, 24(5), 1157-1163.

Israel Ministry of Environmental Protection. (2005). *Kishon River*. Retrieved April 20, 2009, from http://www.sviva.gov.il/Enviroment/bin/en.jsp?enPage=e_BlankPage&enDisplay=view&enDispWhat=Object&enDispWho=Articals^l2074&enZone=Examples_River

Jensen, J.R. (2007) *Remote sensing of the environment* (2nd ed.).New Jersey: Pearson Prentice Hall.

Jha, R., Ojha, C.S.P., & Bhatia, K.K.S. (2007). *Development of refined BOD and DO models for highly polluted Kali River in India.* Journal of Environmental Engineering, 133(8), 839-852.

Karydis, M., & Chatzichristofas, M. (2003). Coastal eutrophication in the Mediterranean marine environment: A short review. *Proceedings of the 8th International Conference on Environmental Science and Technology, Greece ,A,426-430.*

Kenneth, D., Black, K.D., & Shimmield, G.B. (Eds). (2003). *Biogeochemistry of marine systems. Oxford: Blackwell Publishing LTD.*

Kershaw, S., & Cundy, A. (2004). *Oceanography: An earth science perspective*. New York: Routledge

Kirk, J.T.O. (1994). *Light and photosynthesis in aquatic ecosystems (2nd ed.)*. New York: Cambridge University Press.

Kishon River Authority. (2007).*Annual Report*. Retrieved April 01, 2009, from http://www.kishon.org.il/media/File/report07.pdf.

Klein, M., Zviely, D., Kit, E., & Shteinman, B. *Sediment transport along the coast of Israel: Examination of fluorescent sand traces.* Journal of Coastal Research, 23(6), 1462-1470.

Kress, N., & Herut, B. (1998). *Hypernutrification in the oligotrophic Eastern Mediterranean: A study in Haifa Bay (Israel).* Estuarine, Coastal and Shelf Science, 46(5), 645-656.

Krom, M.D., Herut, B., & Mantoura, R.F.C. (2004). *Nutrient budget for the Eastern Mediterranean: Implications for phosphorus limitation.* Limnology and Oceanography, 49(5), 1582-1592.

Malanotte-Rizzoli, P. (2008). *The oceanic circulation of the Mediterranean Sea* [PDF Slides].Retrieved February 5, 2009, from http://www.medclivar.eu/workshopdocs/presentations/Day1_OpeningTalk_Malanotte-Rizzoli.pdf

McCuen, H. (1998).*Hydrology Analysis and Design (2nd* ed). New Jersey: Prentice-Hall.

Michelakaki, M., & Kitisiou, D. (2005). *Estimation of anisotropies in chlorophyll a spatial distributions based on satellite data and variography*. Global NEST Journal, 17(2), 204-211.

Mobley, C., Stramski, D., Bissett, W.P., & Boss, E. (2004). *Optical modeling of ocean waters: Is the case 1 - case 2 classification still useful?.*The Journal of Oceanography Society, 17(2), 61-67.

Morel, A., & Gentili, B. (2009). *A simple band ratio technique to quantify the colored dissolved and detrital organic material from ocean color remotely sensed data.* Remote Sensing of Environment, 113(5), 998-1011.

Morel, A., & Gordon H.R. (1980). *Report on the working group on ocean color*. Boundary Layer Meterol, 18, 343-355.

Morel, A., & Prieur, L. (1977) *Analysis of variation in ocean color.* Limnology and Oceanography, 22(4), 709-722.

National Aeronautics and Space Administration. (2009). *The Enhanced Thematic Mapper Plus*. Retrieved May 05, 2009, from http://landsat.gsfc.nasa.gov/about/etm+.html

National Marine Environmental Monitoring Program. (2004). *Environmental quality of Israel's Mediterranean coastal waters in 2004*. Retrieved April 2, 2009, from http://isramar.ocean.org.il/report.asp

Nixon, S.W. (1995). Coastal marine eutrophication: Definition, social causes and future concerns, OPHELIA, 41, 199-219.

O'Reilly, J.O., Maritorena, S., Mitchell, B.G., Siegel, D.A., Carder, K. L., Garver., et al. (1998). *Ocean color chlorophyll algorithms for SeaWiFS.* J. Geophys. Res, 103 (C11), 24,937-24,953.

Schlarbaum, T., Mara, P., Bahlmann, E., & Emeis. K. (2008). Nitrogen isotope investigation in the Eastern Mediterranean Sea [Abstract]. *Geophysical Research Abstracts*. 10.

Orr, M., *Image processing and spatial analysis of satellite imagery for geobiophysical modeling of sources for increased sediment yield in the Greenup pool of the Ohio River*. Unpublished master's thesis, Marshall University, Huntington. Retrieved September 1, 2008, from Dissertation and Thesis database.

Pacciaroni, M., & Crispi, G. (2007). *Chlorophyll signatures and nutrient cycles in the Mediterranean Sea: A model sensitivity study to nitrogen and phosphorous atmospheric inputs.* Biogeosciences Discussions, 4 (2), 909-959.Patience, M. (2006, September 6). *In focus: Haifa.* BBC News. Retrieved March 31, 2009, from http://news.bbc.co.uk/1/hi/world/middle_east/5318424.stm.

Pearl, H.W. (1997). *Coastal eutrophication and harmful algal blooms: Importance of atmospheric deposition and ground water as "new" nitrogen and other nutrient source.* Limnology and. Oceanography, 42(5, part 2), 1154-1165.

Pearl, H. W., & Whitall D. R. (1999). *Anthropogenically-derived Atmospheric Nitrogen Deposition, Marine Eutrophication and Harmful Algal Bloom expansion: Is there a Link?.* Ambio, 2(4), 307-311.

Perlin, A., & Kit, E. (1999). *Longshore sediment transport on Mediterranean coast of Israel.* Journal of Waterway, Port, Coastal, and Ocean Engineering, 125(2), 80-87.

Purkis, S. (2004). *Calibration of satellite images of reef environments*. Amsterdam: Vrije Universiteit.

Sathyendranath, S., Prieur, L., & Morel, A. (1989). *A three-component model of ocean color and its application to remote sensing of phytoplankton pigments in coastal waters*. International Journal of Remote Sensing, 10(8), 1373-1394.

Sathyendranath, S., Platt, T., Horne E.P.W., Harrioson, W. G., Ulloa, O., Outerbridge., et al. (1991). *Estimation of new production in the ocean by compound remote sensing.* Nature, 353, 129-133.

Seidel, K., & Martinec, J. (2004).*Remote sensing in snow hydrology: Runoff modeling, effect of climate change.* New York: Springer.

Singer, A. (2007). *The soils of Israel*. New York: Springer

Sudarshana, R. (1985). *Gelbstoff-the interfering yellow substance in the chlorophyll remote sensing*. Journal of the Indian Society of Remote Sensing, 13(2), 53-60.

Yacobi, Y.Z., Zohary, T., Kress, N., Hecht, A., Waiser, M., Wood, A.M., et al. (1995). *Chlorophyll distribution throughout the southeastern Mediterranean in relation to the physical structure of the water mass.* Journal of Marine Science, 6(3), 179-190.